

An Online Efficient Two-Scale Reduced Basis Approach for the Localized Orthogonal Decomposition *

Tim Keil[†], Stephan Rave[†]

November 17, 2021

Abstract

We are concerned with employing Model Order Reduction (MOR) to efficiently solve parameterized multiscale problems using the Localized Orthogonal Decomposition (LOD) multiscale method. Like many multiscale methods, the LOD follows the idea of separating the problem into localized fine-scale subproblems and an effective coarse-scale system derived from the solutions of the local problems. While the Reduced Basis (RB) method has already been used to speed up the solution of the fine-scale problems, the resulting coarse system remained untouched, thus limiting the achievable speed up. In this work we address this issue by applying the RB methodology to a new two-scale formulation of the LOD. By reducing the entire two-scale system, this two-scale Reduced Basis LOD (TSRBLOD) approach, yields reduced order models that are completely independent from the size of the coarse mesh of the multiscale approach, allowing an efficient approximation of the solutions of parameterized multiscale problems even for very large domains. A rigorous and efficient a posteriori estimator bounds the model reduction error, taking into account the approximation error for both the local fine-scale problems and the global coarse-scale system.

Keywords: model order reduction, localized orthogonal decomposition, multiscale problems, reduced basis method, a posteriori error estimation, two-scale formulation

AMS Mathematics Subject Classification: 35J20, 65N15, 65N30

1 Introduction

The numerical approximation of partial differential equations that exhibit multiscale structures has many applications in the natural sciences. Typical examples are, for instance, the simulation of composite materials or of flow in porous media. Due to the different spatial or temporal scales at which the physics in such problems are modeled, a direct solution with standard methods such as finite elements is often prohibitively expensive, as very fine meshes over large computational domains are required to resolve all relevant features.

Numerical multiscale methods are designed to overcome this issue by resolving the microstructures only locally to solve small cell problems that yield the fine-scale information required to build an effective coarse-scale system, which then can be solved with modest computational effort. Some of these multiscale methods, such as the Heterogeneous Multiscale Method (HMM) [40], are based on ideas from mathematical homogenization and aim at computing effective coefficients for an appropriate coarse-scale equation. Other approaches, such as the Multiscale Finite Element Method (MsFEM) [24, 15] or the Generalized Finite Element Method (GFEM) [8], instead construct coarse-scale elements that incorporate the local fine-scale features of the solution and then approximate the solution in the space spanned by these multiscale elements.

The Localized Orthogonal Decomposition (LOD) [28], which itself is based on the Variational Multiscale Method (VMM) [25], instead makes use of a splitting of the full fine-scale approximation

***Funding:** The authors acknowledge funding by the Deutsche Forschungsgemeinschaft under Germany's Excellence Strategy EXC 2044 390685587, Mathematics Münster: Dynamics – Geometry – Structure. The first author also acknowledges funding by the DFG contract OH 98/11-1.

[†]Mathematics Münster, Westfälische Wilhelms-Universität Münster, Einsteinstr. 62, D-48149 Münster, {tim.keil, stephanrave}@uni-muenster.de

space into a negligible fine-scale component and an orthogonal multiscale space in which the solution is sought. This multiscale space is then approximated by computing localized approximations of the orthogonal projection into the finescale space (corrector problems). For an extensive overview of the LOD, we refer to [29] and the references therein. In this work we consider a Petrov–Galerkin formulation of the LOD [16], which has lower storage and communication requirements for the computed fine-scale data in comparison to the original Galerkin formulation.

Many problems modeled with partial differential equations include parameters which need to be varied, e.g., to find an optimal choice of parameter values w.r.t. some cost functional. Due to the large costs of repeatedly solving the problem for different parameters in such workflows, Model Order Reduction (MOR) techniques are often used to replace the model at hand by a quickly evaluable surrogate. In this work we consider Reduced Basis (RB) methods, which build such a Reduced Order Model (ROM) by projecting the model equations onto a problem adapted subspace spanned by solutions of the Full Order Model (FOM) for appropriately selected *snapshot* parameters. For a detailed overview and discussion on RB methods, we refer to the monographs [22, 39] and the tutorial introduction [17].

For large, parameterized multiscale problems, RB methods need to be combined with numerical multiscale methods, as otherwise the solution of the FOM for a single snapshot parameter might already be computationally infeasible. One possible approach is to speed up the solution of the individual cell problems using RB techniques, as is done in [11] in the context of numerical homogenization, in [1, 2, 3, 4, 5] for the HMM, in [14, 23, 32] for the MsFEM, or in [6] for the LOD. This approach is applicable both for problems, where the fine-scale data variation over the domain is parameterized, resulting in a single ROM for all cell problems [1, 2, 3, 4, 5, 11, 23], or for general parameterized problems, where for each individual cell problem a dedicated ROM is built [6, 32]. Some recent works have considered the case where the multiscale data varies only in some cells, e.g., caused by perturbations, by a sequence of modification over time or by other parameterizations, such that individual fine-scale solutions can be reused [19, 21, 27] or a ROM can be built in case of parameterized perturbations [31].

All these approaches have in common that, while the constructed surrogates are independent of the resolution of the fine-scale mesh, the effort for their evaluation still scales with the size of the used coarse mesh. Hence, if the coarse mesh itself is large, the repeated assembly and solution of the coarse system still can become a computational bottleneck. Further, the influence of the approximation error of the cell problem ROMs on the coarse system is not rigorously controlled.

In this work we introduce a new two-scale reduced basis method for the LOD (TSRBLOD) that takes both the local corrector problems as well as the coarse-scale problem into account to produce a single small-size ROM that no longer requires explicit solutions of local subproblems in the on-line phase. The model is constructed based on a new two-scale formulation of the LOD as a single variational problem, inspired by the theory of two-scale convergence in mathematical homogenization [7]. As the computation of solution snapshots for this model would still be computationally expensive, we combine this formulation with a preceding reduction of the fine-scale corrector problems similar to the RBLOD approach in [6]. Rigorous and efficient a posteriori bounds derived from the two-scale formulation control the error over this entire two-stage reduction process.

While our two-scale formulation of the LOD is new, an online-efficient RB-ROM for locally periodic homogenization problems was developed for the HMM in [34, 35, 36] based on the two-scale formulation in [33]. Further, we mention localized MOR techniques [13], which can also be employed to obtain online-efficient ROMs for large multiscale problems. Whereas numerical multiscale methods build on the idea of scale separation and computing effective global systems from local information, these methods are usually based on the idea of decomposing the computational domain and deriving a globally coupled ROM from local ROMs associated with the domain decomposition.

This paper is organized as follows. In section 2 we introduce the considered model problem, after which we briefly review the LOD method in section 3. Section 4 is devoted to our two-scale formulation of the LOD. In particular, we prove inf-sup stability of the introduced two-scale bilinear form, from which we derive error bounds for the two-scale system. In section 5 we detail our new two-stage reduction approach for the LOD based on this two-scale formulation. The numerical experiments in section 6 show the efficiency of the method, in particular for large problems. We end with some concluding remarks in section 7.

2 Problem formulation

Let $\mathcal{P} \subset \mathbb{R}^p$, $p \in \mathbb{N}$ be a parameter space and $\Omega \in \mathbb{R}^d$ a bounded Lipschitz domain. We consider the following prototypical parameterized elliptic partial differential equation: for a fixed parameter $\mu \in \mathcal{P}$, find u_μ such that

$$(1) \quad \begin{aligned} -\nabla \cdot A_\mu(x) \nabla u_\mu(x) &= f(x), & \text{in } \Omega, \\ u_\mu(x) &= 0, & x \in \partial\Omega. \end{aligned}$$

We assume that the parameter-dependent coefficient field A_μ has a multiscale structure that renders a direct solution of (1) using, e.g., finite elements computationally infeasible due to the high mesh resolution required to resolve all features of A_μ .

Further, we assume $A_\mu \in L^\infty(\Omega, \mathbb{R}^{d \times d})$ to be symmetric and uniformly elliptic w.r.t. x and μ , i.e., there exist $0 < \alpha \leq \beta < \infty$ such that

$$(2) \quad \forall \mu \in \mathcal{P} \quad \forall x \in \Omega \quad \forall \xi \in \mathbb{R}^d : \quad \alpha |\xi|^2 \leq \xi^T \cdot A_\mu(x) \cdot \xi \leq \beta |\xi|^2,$$

and we let $\kappa := \beta/\alpha$ be the maximum contrast of A_μ . Moreover, let $f \in L^2(\Omega)$.

We consider the weak formulation of (1): for $\mu \in \mathcal{P}$, we seek $u_\mu \in V := H_0^1(\Omega)$ such that

$$(3) \quad a_\mu(u_\mu, v) = F(v) \quad \forall v \in V,$$

where

$$a_\mu(u, v) := \int_{\Omega} (A_\mu(x) \nabla u(x)) \cdot \nabla v(x) \, dx \quad \text{and} \quad F(v) := \int_{\Omega} f(x) v(x) \, dx.$$

Due to our assumptions, a_μ is a continuous, coercive bilinear form on V and $F \in V'$, s.t. (3) admits a unique solution by the Lax-Milgram theorem.

As a final assumption, which will be required in section 5 to obtain an online-efficient reduced order model, we assume parameter-separability of A_μ , i.e., we assume A_μ to have a decomposition $A_\mu = \sum_{q=1}^Q \theta_q(\mu) A_q$ with non-parametric $A_q \in L^\infty(\Omega)$ and arbitrary $\theta_q : \mathcal{P} \rightarrow \mathbb{R}$. This gives rise to the corresponding decomposition

$$(4) \quad a_\mu(u, v) = \sum_{q=1}^Q \theta_q(\mu) a_q(u, v),$$

of a_μ , where $a_q(u, v) := \int_{\Omega} (A_q(x) \nabla u(x)) \cdot \nabla v(x) \, dx$. In case A_μ does not exhibit such a decomposition, empirical interpolation [9] can be used to obtain an approximate decomposition of A_μ .

Finally, for $v \in V = H_0^1(\Omega)$ we introduce the following norms:

$$\|v\|_1 := \int_{\Omega} |\nabla v(x)| \, dx, \quad \|v\|_{a,\mu} := \int_{\Omega} |A_\mu^{1/2} \nabla v(x)| \, dx.$$

Note that $\|\cdot\|_1$ is a norm on V due to Friedrich's inequality.

We remark that our approach can be easily generalized to parametric f and other boundary conditions.

3 Localized Orthogonal Decomposition

In this section we review the basic concepts of the LOD. The general idea of the LOD is to decompose the solution space into a subspace V_h^f of negligible fine-scale variations and an a_μ -orthogonal low-dimensional coarse space of multiscale functions, in which the solution is approximated. This multiscale space is constructed by computing suitable fine-scale corrections $\mathcal{Q}_\mu(u_H)$ of functions from a given coarse finite-element space V_H . Due to the dampening of high-frequency oscillations by a_μ , these corrections can then be approximated by the solution of decoupled localized corrector problems.

In recent years, there have been various formulations of the LOD in terms of localization, interpolation, approximation schemes and applications. Since we are concerned with the case where storage restrictions may prevent to store explicit solutions of the corrector problems, we focus on the Petrov–Galerkin version of the LOD (PG–LOD) [16], which is favorable in this respect. For further background, we refer to [29].

3.1 Discretization and patches

Let $V_h \subset V$ be a conforming finite-element space of dimension N_h , and let \mathcal{T}_h be the corresponding shape regular mesh over the computational domain Ω . We assume that the mesh size h is chosen such that all features of A_μ are resolved, making a global solution within V_h infeasible. Further, we assume to be given a coarse mesh \mathcal{T}_H with mesh size $H \gg h$ that is aligned with \mathcal{T}_h , and let

$$V_H := V_h \cap \mathcal{P}_1(\mathcal{T}_H),$$

where $\mathcal{P}_1(\mathcal{T}_H)$ denotes \mathcal{T}_H -piecewise affine functions that are continuous on Ω . We denote the dimension of V_H by N_H .

For an arbitrary set $\omega \subseteq \Omega$, we define coarse grid element patches $U_k(\omega) \subset \Omega$ of size $0 \leq k \in \mathbb{N}$ by

$$U_0(\omega) := \omega, \quad \text{and} \quad U_{k+1}(\omega) := \text{Int} \left(\overline{\bigcup \left\{ T \in \mathcal{T}_H \mid \overline{U_k(\omega)} \cap \overline{T} \neq \emptyset \right\}} \right),$$

where $\text{Int}(X)$ is the interior of the set X . For a given patch size k , let

$$C_{k,\text{ovl}} := \max_{x \in \Omega} \#\{T \in \mathcal{T}_H \mid x \in U_k(T)\}$$

be the maximum number of element patches overlapping in a single point of Ω .

3.2 Localized multiscale space

In order to define the fine-scale space V_h^f , we consider a (quasi-)interpolation operator $\mathcal{I}_H : V_h \rightarrow V_H$, and let $V_h^f := \ker(\mathcal{I}_H)$. Multiple choices for such an interpolation operator are possible (see [20, 38] for an overview). In recent literature, using an operator that is based on local L^2 -projections [37] has proven advantageous. However, for the following error analysis we only require that \mathcal{I}_H is linear, $\|\cdot\|_1$ -continuous and idempotent on V_H , i.e.,

$$\begin{aligned} \mathcal{I}_H(v_H) &= v_H & \forall v_H \in V_H, \\ \|\mathcal{I}_H(v_h)\|_1 &\leq C_{\mathcal{I}_H} \|v_h\|_1 & \forall v_h \in V_h. \end{aligned}$$

Next, we define the fine-scale corrections $\mathcal{Q}_\mu(v) \in V_h^f$, for a given $v_h \in V_h$, to be the solution of

$$a_\mu(\mathcal{Q}_\mu(v_h), v^f) = a_\mu(v_h, v^f) \quad \forall v^f \in V_h^f.$$

Thus, $\mathcal{Q}_\mu(v_h)$ is the a_μ -orthogonal projection of v_h onto V_h^f , and the multiscale space

$$V_{H,\mu}^{\text{ms}} := (I - \mathcal{Q}_\mu)(V_H)$$

is the a_μ -orthogonal complement of V_h^f in V_h , i.e., $V_h = V_{H,\mu}^{\text{ms}} \oplus_{a_\mu} V_h^f$.

However, even when v_h has a small local support, $\mathcal{Q}_\mu(v_h)$ will have global support, and its computation will require the same effort as a global solution of (3) in V_h . Thus, we approximate $\mathcal{Q}_\mu(v_h)$ using localized correctors $\mathcal{Q}_{k,\mu}^T(v_h) \in V_{h,k,T}^f$ in the patch-restricted fine-scale spaces $V_{h,k,T}^f := V_h^f \cap H_0^1(U_k(T))$ given by

$$(5) \quad a_\mu(\mathcal{Q}_{k,\mu}^T(v_h), v^f) = a_\mu^T(v_h, v^f) \quad \forall v^f \in V_{h,k,T}^f,$$

where a_μ^T denotes the bilinear form obtained by restricting the integration domain in the definition of a_μ to $T \in \mathcal{T}_H$. We then define the localized corrector by

$$(6) \quad \mathcal{Q}_{k,\mu} := \sum_{T \in \mathcal{T}_H} \mathcal{Q}_{k,\mu}^T,$$

and the localized multiscale space $V_{H,k,\mu}^{\text{ms}}$ by

$$V_{H,k,\mu}^{\text{ms}} := (I - \mathcal{Q}_{k,\mu})(V_H).$$

Due to the exponential decay of the correctors [28], we choose a patch localization parameter of $k \approx |\log H|$ to obtain a sufficient approximation.

3.3 Petrov–Galerkin projection

After computing $V_{H,k,\mu}^{\text{ms}}$, we determine an approximation of u_μ in this N_H -dimensional multiscale space via Petrov-Galerkin projection. I.e., we let $u_{H,k,\mu}^{\text{ms}} \in V_{H,k,\mu}^{\text{ms}}$ be the solution of

$$(7) \quad a_\mu(u_{H,k,\mu}^{\text{ms}}, v_H) = F(v_H) \quad \forall v_H \in V_H.$$

To ensure that (7) has a unique solution, inf-sup stability of a_μ w.r.t. $V_{H,k,\mu}^{\text{ms}}$ and V_H is required, which has been shown in [16, 21]. Compared to these references, we use a slightly different definition of the inf-sup stability constant for (7) by using $\|\cdot\|_1$ instead of $\|\cdot\|_{a,\mu}$ for the test space:

$$\gamma_k := \inf_{0 \neq w_H \in V_H} \sup_{0 \neq v_H \in V_H} \frac{a_\mu(w_H - \mathcal{Q}_{k,\mu}^T(w_H), v_H)}{\|w_H - \mathcal{Q}_{k,\mu}^T(w_H)\|_{a,\mu} \|v_H\|_1}.$$

For k large enough, we have that

$$(8) \quad \gamma_k \approx \alpha^{1/2} C_{\mathcal{I}_H}^{-1},$$

which can be proven with a simple modification of the argument in [21, Section 4]. In particular, w.l.o.g. we assume that $\gamma_k \leq \alpha^{1/2}$.

Writing the solution of (7) as $u_{H,k,\mu}^{\text{ms}} = u_{H,k,\mu} - \mathcal{Q}_{k,\mu}(u_{H,k,\mu})$ with $u_{H,k,\mu} \in V_H$, we have the following a priori estimate, which was first shown in [16].

Theorem 3.1 (A priori convergence result for the PG-LOD). *For a fixed parameter $\mu \in \mathcal{P}$, let $u_{h,\mu} \in V_h$ be the finite-element solution of (3) given by*

$$a_\mu(u_{h,\mu}, v_h) = F(v_h) \quad \forall v_h \in V_h.$$

Then it holds that

$$\|u_{h,\mu} - u_{H,k,\mu}\|_{L^2} + \|u_{h,\mu} - u_{H,k,\mu}^{\text{ms}}\|_1 \lesssim (H + \theta^k k^{d/2}) \|f\|_{L^2(\Omega)},$$

with $0 < \theta < 1$ independent of H and k , but dependent on the contrast κ .

Although our setting is slightly different to the one in [16] (in terms of localization and interpolation), the proof can still be followed analogously. For a detailed discussion on the decay variable θ , we refer to [20, 21, 28].

3.4 Computational aspects

In order to solve (7), we need to solve multiple corrector problems (5) for every $T \in \mathcal{T}_H$. These correctors are then used to assemble a localized multiscale matrix \mathbb{K}_μ given by

$$(9) \quad \mathbb{K}_\mu := \sum_{T \in \mathcal{T}_H} \mathbb{K}_{T,\mu}, \quad (\mathbb{K}_{T,\mu})_{ji} := (A_\mu(\chi_T \nabla - \nabla \mathcal{Q}_{k,\mu}^T) \phi_i, \nabla \phi_j)_{U_k(T)},$$

where χ_T denotes the indicator function on T and ϕ_i the finite-element basis functions of V_H . Solving (7) then is equivalent to solving the linear system

$$(10) \quad \mathbb{K}_\mu \cdot \underline{u}_{H,k,\mu}^{\text{ms}} = \mathbb{F},$$

where $\mathbb{F}_i := F(\phi_i)$, and $\underline{u}_{H,k,\mu}^{\text{ms}} \in \mathbb{R}^{N_H}$ is the vector of coefficients of $u_{H,k,\mu}^{\text{ms}}$ w.r.t. the basis of $V_{H,k,\mu}^{\text{ms}}$ corresponding to the finite-element basis ϕ_i .

Compared to Galerkin projection onto $V_{H,k,\mu}^{\text{ms}}$, the system matrix \mathbb{K}_μ of the Petrov-Galerkin formulation has a smaller sparsity pattern, and we need less computational work to assemble the matrix. Every localized corrector and thus each local contribution to \mathbb{K}_μ can be computed in parallel without any communication and can be deleted after the contribution $\mathbb{K}_{T,\mu}$ has been computed. In particular, note that the local contribution matrices $\mathbb{K}_{T,\mu}$ only have non-zeros in columns i for which $T \subseteq \text{supp } \phi_i$.

Overall, to compute the LOD solution the following steps are required:

1. For every $T \in \mathcal{T}_H$: Compute $\mathcal{Q}_{k,\mu}^T(\phi_i)$ by solving (5) for each i s.t. $T \subseteq \text{supp } \phi_i$. Assemble $\mathbb{K}_{T,\mu}$ according to (9).
2. Assemble the localized multiscale stiffness matrix $\mathbb{K}_\mu = \sum_{T \in \mathcal{T}_H} \mathbb{K}_{T,\mu}$ from the local contributions computed in step 1.
3. Solve equation (10) to compute $\underline{u}_{H,k,\mu}^{\text{ms}}$.

In general, neither of the steps 1–3 is computational negligible, and each of these steps has to be repeated to obtain a solution for a new $\mu \in \mathcal{P}$. Note that step 1 requires computations on the fine-scale level whereas steps 2 and 3 solely depend on the size of the coarse mesh \mathcal{T}_H . In [6], RB approximations of the local corrector problems were introduced to obtain a model that is independent from the size of \mathcal{T}_h . However, for large \mathcal{T}_H , the costs of solving the reduced corrector problems in step 1 and the further computations in steps 2 and 3 still can be significant. The two-scale reduction approach introduced in this work takes all computational steps into account and yields a reduced order model that is independent from the sizes of both \mathcal{T}_h and \mathcal{T}_H .

4 Two-scale formulation of the PG–LOD

We formulate the PG–LOD method in a two-scale formulation. In particular, we aim at considering the PG–LOD solution as the solution of one single system where the coarse system (7) and all fine scale corrections (5) are solved at the same time. This formulation will be the basis for the Stage 2 ROM constructed in subsection 5.2.

4.1 The two-scale bilinear form

Let \mathfrak{V} denote the two-scale function space given by the direct sum of Hilbert spaces

$$\mathfrak{V} := V_H \oplus V_{h,k,T_1}^f \oplus \cdots \oplus V_{h,k,T_{|\mathcal{T}_H|}}^f.$$

In particular, for $\mathbf{u} = (u_H, u_{T_1}^f, \dots, u_{T_{|\mathcal{T}_H|}}^f) \in \mathfrak{V}$ we define the two-scale H^1 -norm of \mathbf{u} by

$$\|\mathbf{u}\|_1^2 := \|u_H\|_1^2 + \sum_{T \in \mathcal{T}_H} \|u_T^f\|_1^2.$$

On this space, we define the two-scale bilinear form $\mathfrak{B}_\mu \in \text{Bil}(\mathfrak{V})$ given by

$$\begin{aligned} \mathfrak{B}_\mu \left((u_H, u_{T_1}^f, \dots, u_{T_{|\mathcal{T}_H|}}^f), (v_H, v_{T_1}^f, \dots, v_{T_{|\mathcal{T}_H|}}^f) \right) := \\ a_\mu(u_H - \sum_{T \in \mathcal{T}_H} u_T^f, v_H) + \rho^{1/2} \sum_{T \in \mathcal{T}_H} a_\mu(u_T^f, v_T^f) - a_\mu^T(u_H, v_T^f), \end{aligned}$$

with a stabilization parameter $\rho \geq 1$ that will be chosen later. Further let $\mathfrak{F} \in \mathfrak{V}'$ be given by

$$\mathfrak{F} \left((v_H, v_{T_1}^f, \dots, v_{T_{|\mathcal{T}_H|}}^f) \right) := F(v_H),$$

and define the two-scale solution $\mathbf{u}_\mu \in \mathfrak{V}$ of the PG–LOD by the variational problem

$$(11) \quad \mathfrak{B}_\mu(\mathbf{u}_\mu, \mathbf{v}) = \mathfrak{F}(\mathbf{v}) \quad \forall \mathbf{v} \in \mathfrak{V}.$$

We show, that (11) is equivalent to the original formulation (5), (7):

Proposition 4.1. *The two-scale solution $\mathbf{u}_\mu \in \mathfrak{V}$ of (11) is uniquely determined and given by*

$$(12) \quad \mathbf{u}_\mu = \left[u_{H,k,\mu}, \mathcal{Q}_{k,\mu}^{T_1}(u_{H,k,\mu}), \dots, \mathcal{Q}_{k,\mu}^{T_{|\mathcal{T}_H|}}(u_{H,k,\mu}) \right].$$

Proof. With \mathbf{u}_μ as in (12) we have for any $\mathbf{v} = (v_H, v_{T_1}^f, \dots, v_{T_{|\mathcal{T}_H|}}^f)$

$$\mathfrak{B}_\mu(\mathbf{u}_\mu, \mathbf{v}) = a_\mu(u_{H,k,\mu} - \sum_{T \in \mathcal{T}_H} \mathcal{Q}_{k,\mu}^T(u_{H,k,\mu}), v_H)$$

$$\begin{aligned}
& + \rho^{1/2} \sum_{T \in \mathcal{T}_H} a_\mu(\mathcal{Q}_{k,\mu}^T(u_{H,k,\mu}), v_T^f) - a_\mu^T(u_{H,k,\mu}, v_T^f) \\
& = F(v_H) = \mathfrak{F}(\mathbf{v}),
\end{aligned}$$

where we have used the definition of $\mathcal{Q}_{k,\mu}^T(u_{H,k,\mu})$ to eliminate the sum over \mathcal{T}_H , the definition of $\mathcal{Q}_{k,\mu}$ (6) and the definition of $u_{H,k,\mu}$ (7).

To show that \mathbf{u}_μ is the only solution of (12), it suffices to show that $\mathfrak{B}_\mu(\mathbf{u}, \mathbf{v}) = 0$ for all $\mathbf{v} \in \mathfrak{V}$ implies $\mathbf{u} = (u_H, u_{T_1}^f, \dots, u_{T_{|\mathcal{T}_H|}}^f) = 0$. For that, first note that for $1 \leq i \leq T_{|\mathcal{T}_H|}$ and each $v_{T_i}^f \in V_{h,k,T}^f$ we have:

$$a_\mu(u_{T_i}^f, v_{T_i}^f) - a_\mu^T(u_H, v_{T_i}^f) = \rho^{-1/2} \cdot \mathfrak{B}_\mu(\mathbf{u}, (0, \dots, 0, v_{T_i}^f, 0, \dots, 0)) = 0,$$

hence, $u_{T_i}^f = \mathcal{Q}_{k,\mu}^T(u_H)$. This implies $a_\mu(u_H - \mathcal{Q}_{k,\mu}(u_H), v_H) = \mathfrak{B}_\mu(\mathbf{u}, (v_H, 0, \dots, 0)) = 0$ for all $v_H \in V_H$, which means $u_H = 0$ due to the inf-sup stability of the PG-LOD bilinear form. However, $u_H = 0$ implies $\mathcal{Q}_{k,\mu}^T(u_H) = 0$ for all $T \in \mathcal{T}_H$. \square

4.2 Analysis of the two-scale bilinear form

We introduce two weighted norms $\|\cdot\|_{a,\mu}$, $\|\cdot\|_{1,\mu}$ on \mathfrak{V} , w.r.t. which we will show the inf-sup stability of \mathfrak{B}_μ and derive approximation error bounds. For arbitrary $\mathbf{u} = (u_H, u_{T_1}^f, \dots, u_{T_{|\mathcal{T}_H|}}^f) \in \mathfrak{V}$ these norms are given by

$$\begin{aligned}
\|\mathbf{u}\|_{a,\mu}^2 & := \|u_H - \sum_{T \in \mathcal{T}_H} u_T^f\|_{a,\mu}^2 + \rho \sum_{T \in \mathcal{T}_H} \|\mathcal{Q}_{k,\mu}^T(u_H) - u_T^f\|_{a,\mu}^2, \\
\|\mathbf{u}\|_{1,\mu}^2 & := \|u_H\|_1^2 + \rho \sum_{T \in \mathcal{T}_H} \|\mathcal{Q}_{k,\mu}^T(u_H) - u_T^f\|_1^2.
\end{aligned}$$

Proposition 4.2. $\|\cdot\|_{a,\mu}$ and $\|\cdot\|_{1,\mu}$ are norms on \mathfrak{V} for all $\mu \in \mathcal{P}$.

Proof. Since $\mathbf{u} \mapsto u_H - \sum_{T \in \mathcal{T}_H} u_T^f$ and $\mathbf{u} \mapsto \mathcal{Q}_{k,\mu}^T(u_H) - u_T^f$ are linear, the pull-back norms $\|u_H - \sum_{T \in \mathcal{T}_H} u_T^f\|_{a,\mu}$ and $\|\mathcal{Q}_{k,\mu}^T(u_H) - u_T^f\|_{a,\mu}$ are semi-norms on \mathfrak{V} . Hence, $\|\cdot\|_{a,\mu}$ is a semi-norm on \mathfrak{V} as well.

Further, we have $\|u_H\|_1 = \|\mathcal{I}_H(u_H - \sum_{T \in \mathcal{T}_H} u_T^f)\|_1 \leq C_{\mathcal{I}_H} \|u_H - \sum_{T \in \mathcal{T}_H} u_T^f\|_1 \leq C_{\mathcal{I}_H} \alpha^{-1/2} \|u_H - \sum_{T \in \mathcal{T}_H} u_T^f\|_{a,\mu}$, so $\|\mathbf{u}\|_{a,\mu} = 0$ implies $u_H = 0$. This in turn implies $\|u_T^f\|_{a,\mu} = \|\mathcal{Q}_{k,\mu}^T(u_H) - u_T^f\|_{a,\mu} = 0$ for all $T \in \mathcal{T}_H$, so $\mathbf{u}_\mu = 0$. Hence, $\|\cdot\|_{a,\mu}$ is indeed a norm on \mathfrak{V} . The argument for $\|\cdot\|_{1,\mu}$ is similar. \square

We are going to show that $\|\cdot\|_{a,\mu}$ and $\|\cdot\|_{1,\mu}$ are equivalent norms, for which we require some technical results.

Lemma 4.3. Let $v_T^f \in V_{h,k,T}^f$ for each $T \in \mathcal{T}_H$ be given. Then we have:

$$\left\| \sum_{T \in \mathcal{T}_H} v_T^f \right\|_1^2 \leq C_{k,\text{ovl}} \sum_{T \in \mathcal{T}_H} \|v_T^f\|_1^2 \quad \text{and} \quad \left\| \sum_{T \in \mathcal{T}_H} v_T^f \right\|_{a,\mu}^2 \leq C_{k,\text{ovl}} \sum_{T \in \mathcal{T}_H} \|v_T^f\|_{a,\mu}^2.$$

Proof. Using Jensen's inequality, we have:

$$\begin{aligned}
\left\| \sum_{T \in \mathcal{T}_H} v_T^f \right\|_{a,\mu}^2 & = \int_\Omega \left| \sum_{T \in \mathcal{T}_H} A_\mu^{1/2}(x) \nabla v_T^f(x) \right|^2 dx \\
& \leq \int_\Omega C_{k,\text{ovl}} \cdot \sum_{T \in \mathcal{T}_H} |A_\mu^{1/2}(x) \nabla v_T^f(x)|^2 dx = C_{k,\text{ovl}} \sum_{T \in \mathcal{T}_H} \|v_T^f\|_{a,\mu}^2.
\end{aligned}$$

The proof for $\|\cdot\|_1$ is the same. \square

Lemma 4.4. For arbitrary $u_H \in V_H$ we have

$$\left(\sum_{T \in \mathcal{T}_H} \|\mathcal{Q}_{k,\mu}^T(u_H)\|_{a,\mu}^2 \right)^{1/2} \leq \|u_H\|_{a,\mu}.$$

Proof. By definition of $\mathcal{Q}_{k,\mu}^T$ we have

$$\begin{aligned}
\sum_{T \in \mathcal{T}_H} \|\mathcal{Q}_{k,\mu}^T(u_H)\|_{a,\mu}^2 &= \sum_{T \in \mathcal{T}_H} a_\mu(\mathcal{Q}_{k,\mu}^T(u_H), \mathcal{Q}_{k,\mu}^T(u_H)) = \sum_{T \in \mathcal{T}_H} a_\mu^T(u_H, \mathcal{Q}_{k,\mu}^T(u_H)) \\
&\leq \sum_{T \in \mathcal{T}_H} \left(\int_T |A_\mu^{1/2}(x) \nabla u_H(x)|^2 dx \right)^{1/2} \cdot \left(\int_T |A_\mu^{1/2}(x) \nabla \mathcal{Q}_{k,\mu}^T(u_H)(x)|^2 dx \right)^{1/2} \\
&\leq \left(\sum_{T \in \mathcal{T}_H} \int_T |A_\mu^{1/2}(x) \nabla u_H(x)|^2 dx \right)^{1/2} \cdot \left(\sum_{T \in \mathcal{T}_H} \int_T |A_\mu^{1/2}(x) \nabla \mathcal{Q}_{k,\mu}^T(u_H)(x)|^2 dx \right)^{1/2} \\
&\leq \|u_H\|_{a,\mu}^2 \cdot \left(\sum_{T \in \mathcal{T}_H} \|\mathcal{Q}_{k,\mu}^T u_H\|_{a,\mu}^2 \right)^{1/2}.
\end{aligned}$$

Dividing by the second factor yields the claim. \square

Now, we are prepared to show the equivalence of both norms.

Proposition 4.5. $\|\cdot\|_{a,\mu}$ and $\|\cdot\|_{1,\mu}$ are equivalent norms on \mathfrak{V} with the following bounds for every $\mathbf{u} \in \mathfrak{V}$:

$$C_{\mathcal{I}_H}^{-1} \alpha^{1/2} \|\mathbf{u}\|_{1,\mu} \leq \|\mathbf{u}\|_{a,\mu} \leq \sqrt{3}(1 + C_{k,\text{ovl}})^{1/2} \beta^{1/2} \|\mathbf{u}\|_{1,\mu}.$$

Proof. Let $\mathbf{u} = (u_H, u_{T_1}^f, \dots, u_{T_{|\mathcal{T}_H|}}^f)$. To bound $\|\mathbf{u}\|_{1,\mu}$ by $\|\mathbf{u}\|_{a,\mu}$, note that

$$(13) \quad \|u_H\|_1^2 \leq C_{\mathcal{I}_H}^2 \|u_H - \sum_{T \in \mathcal{T}_H} u_T^f\|_1^2 \leq \alpha^{-1} C_{\mathcal{I}_H}^2 \|u_H - \sum_{T \in \mathcal{T}_H} u_T^f\|_{a,\mu}^2,$$

and, using $C_{\mathcal{I}_H} \geq 1$,

$$\rho \sum_{T \in \mathcal{T}_H} \|\mathcal{Q}_{k,\mu}^T(u_H) - u_T^f\|_1^2 \leq \alpha^{-1} C_{\mathcal{I}_H}^2 \rho \sum_{T \in \mathcal{T}_H} \|\mathcal{Q}_{k,\mu}^T(u_H) - u_T^f\|_{a,\mu}^2.$$

To bound $\|\mathbf{u}\|_{a,\mu}$ by $\|\mathbf{u}\|_{1,\mu}$ we use Lemma 4.3, Lemma 4.4 and $\rho \geq 1$ to obtain

$$\begin{aligned}
&\|u_H - \sum_{T \in \mathcal{T}_H} u_T^f\|_{a,\mu}^2 \\
&\leq 3\|u_H\|_{a,\mu}^2 + 3C_{k,\text{ovl}} \sum_{T \in \mathcal{T}_H} \|\mathcal{Q}_{k,\mu}^T(u_H) - u_T^f\|_{a,\mu}^2 + 3C_{k,\text{ovl}} \sum_{T \in \mathcal{T}_H} \|\mathcal{Q}_{k,\mu}^T(u_H)\|_{a,\mu}^2 \\
&\leq 3(1 + C_{k,\text{ovl}}) \|u_H\|_{a,\mu}^2 + 3C_{k,\text{ovl}} \rho \sum_{T \in \mathcal{T}_H} \|\mathcal{Q}_{k,\mu}^T(u_H) - u_T^f\|_{a,\mu}^2 \\
&\leq 3(1 + C_{k,\text{ovl}}) \beta \|u_H\|_1^2 + 3C_{k,\text{ovl}} \beta \rho \sum_{T \in \mathcal{T}_H} \|\mathcal{Q}_{k,\mu}^T(u_H) - u_T^f\|_1^2.
\end{aligned}$$

Adding

$$\rho \sum_{T \in \mathcal{T}_H} \|\mathcal{Q}_{k,\mu}^T(u_H) - u_T^f\|_{a,\mu}^2 \leq \beta \rho \sum_{T \in \mathcal{T}_H} \|\mathcal{Q}_{k,\mu}^T(u_H) - u_T^f\|_1^2$$

to both sides yields the claim. \square

Finally, we show that \mathfrak{B}_μ is $\|\cdot\|_{a,\mu}$ - $\|\cdot\|_1$ inf-sup stable with controllable constants.

Proposition 4.6. *Let*

$$\rho := C_{k,\text{ovl}} \cdot \kappa,$$

then \mathfrak{B}_μ is $\|\cdot\|_{a,\mu}$ - $\|\cdot\|_1$ -continuous and inf-sup stable with the following bounds on the respective constants:

$$\sup_{0 \neq \mathbf{u} \in \mathfrak{V}} \sup_{0 \neq \mathbf{v} \in \mathfrak{V}} \frac{\mathfrak{B}_\mu(\mathbf{u}, \mathbf{v})}{\|\mathbf{u}\|_{a,\mu} \cdot \|\mathbf{v}\|_1} \leq \beta^{1/2} \quad \text{and} \quad \inf_{0 \neq \mathbf{u} \in \mathfrak{V}} \sup_{0 \neq \mathbf{v} \in \mathfrak{V}} \frac{\mathfrak{B}_\mu(\mathbf{u}, \mathbf{v})}{\|\mathbf{u}\|_{a,\mu} \cdot \|\mathbf{v}\|_1} \geq \gamma_k / \sqrt{5}.$$

Proof. We first bound the continuity constant of \mathfrak{B}_μ . To this end, let $\mathbf{u} = (u_H, u_{T_1}^f, \dots, u_{T_{|\mathcal{T}_H|}}^f) \in \mathfrak{V}$ and $\mathbf{v} = (v_H, v_{T_1}^f, \dots, v_{T_{|\mathcal{T}_H|}}^f) \in \mathfrak{V}$ be arbitrary. Then we have

$$\begin{aligned}
\mathfrak{B}_\mu(\mathbf{u}, \mathbf{v}) &= a_\mu(u_H - \sum_{T \in \mathcal{T}_H} u_T^f, v_H) - \rho^{1/2} \sum_{T \in \mathcal{T}_H} (a_\mu(u_T^f, v_T^f) - a_\mu^T(u_H, v_T^f)) \\
&\leq \|u_H - \sum_{T \in \mathcal{T}_H} u_T^f\|_{a,\mu} \|v_H\|_{a,\mu} + \sum_{T \in \mathcal{T}_H} \rho^{1/2} \|u_T^f - \mathcal{Q}_{k,\mu}^T(u_H)\|_{a,\mu} \|v_T^f\|_{a,\mu} \\
&\leq \left[\|u_H - \sum_{T \in \mathcal{T}_H} u_T^f\|_{a,\mu}^2 + \sum_{T \in \mathcal{T}_H} \rho \|u_T^f - \mathcal{Q}_{k,\mu}^T(u_H)\|_{a,\mu}^2 \right]^{1/2} \\
&\quad \cdot \left[\|v_H\|_{a,\mu}^2 + \sum_{T \in \mathcal{T}_H} \|v_T^f\|_{a,\mu}^2 \right]^{1/2} \\
&\leq \|\mathbf{u}\|_{a,\mu} \cdot \beta^{1/2} \cdot \|\mathbf{v}\|_1.
\end{aligned}$$

To prove inf-sup stability, first note that

$$\begin{aligned}
&\|u_H - \sum_{T \in \mathcal{T}_H} u_T^f\|_{a,\mu} \\
&\leq \|u_H - \sum_{T \in \mathcal{T}_H} \mathcal{Q}_{k,\mu}^T(u_H)\|_{a,\mu} + \left\| \sum_{T \in \mathcal{T}_H} (\mathcal{Q}_{k,\mu}^T(u_H) - u_T^f) \right\|_{a,\mu} \\
&\leq \gamma_k^{-1} \sup_{0 \neq v_H \in V_H} \frac{a_\mu(u_H - \sum_{T \in \mathcal{T}_H} \mathcal{Q}_{k,\mu}^T(u_H), v_H)}{\|v_H\|_1} + \left\| \sum_{T \in \mathcal{T}_H} (\mathcal{Q}_{k,\mu}^T(u_H) - u_T^f) \right\|_{a,\mu} \\
&\leq \underbrace{\gamma_k^{-1} \sup_{0 \neq v_H \in V_H} \frac{\mathfrak{B}_\mu(\mathbf{u}, (v_H, 0, \dots, 0))}{\|(v_H, 0, \dots, 0)\|_1}}_A \\
&\quad + \gamma_k^{-1} \sup_{0 \neq v_H \in V_H} \frac{a_\mu(\sum_{T \in \mathcal{T}_H} (\mathcal{Q}_{k,\mu}^T(u_H) - u_T^f), v_H)}{\|v_H\|_1} + \left\| \sum_{T \in \mathcal{T}_H} (\mathcal{Q}_{k,\mu}^T(u_H) - u_T^f) \right\|_{a,\mu} \\
&\leq \gamma_k^{-1} A + \left(\gamma_k^{-1} \sup_{0 \neq v_H \in V_H} \frac{\|v_H\|_{a,\mu}}{\|v_H\|_1} + 1 \right) \left\| \sum_{T \in \mathcal{T}_H} (\mathcal{Q}_{k,\mu}^T(u_H) - u_T^f) \right\|_{a,\mu} \\
&\leq \gamma_k^{-1} A + (\gamma_k^{-1} \beta^{1/2} + 1) C_{k,\text{ovl}}^{1/2} \left(\sum_{T \in \mathcal{T}_H} \|\mathcal{Q}_{k,\mu}^T(u_H) - u_T^f\|_{a,\mu}^2 \right)^{1/2},
\end{aligned}$$

hence:

$$\begin{aligned}
\|\mathbf{u}\|_{a,\mu}^2 &= \|u_H - \sum_{T \in \mathcal{T}_H} u_T^f\|_{a,\mu}^2 + \rho \sum_{T \in \mathcal{T}_H} \|\mathcal{Q}_{k,\mu}^T(u_H) - u_T^f\|_{a,\mu}^2 \\
&\leq 2\gamma_k^{-2} A^2 + (2\gamma_k^{-2} \beta C_{k,\text{ovl}} + 2C_{k,\text{ovl}} + \rho) \sum_{T \in \mathcal{T}_H} \|\mathcal{Q}_{k,\mu}^T(u_H) - u_T^f\|_{a,\mu}^2.
\end{aligned}$$

Further,

$$\begin{aligned}
\left(\sum_{T \in \mathcal{T}_H} \|u_T^f - \mathcal{Q}_{k,\mu}^T(u_H)\|_{a,\mu}^2 \right)^{1/2} &= \frac{\sum_{T \in \mathcal{T}_H} a_\mu(u_T^f - \mathcal{Q}_{k,\mu}^T(u_H), u_T^f - \mathcal{Q}_{k,\mu}^T(u_H))}{(\sum_{T \in \mathcal{T}_H} \|u_T^f - \mathcal{Q}_{k,\mu}^T(u_H)\|_{a,\mu}^2)^{1/2}} \\
&\leq \sup_{v_T^f \in V_{h,k,T}^f} \frac{\sum_{T \in \mathcal{T}_H} a_\mu(u_T^f - \mathcal{Q}_{k,\mu}^T(u_H), v_T^f)}{(\sum_{T \in \mathcal{T}_H} \|v_T^f\|_{a,\mu}^2)^{1/2}} \\
&\leq \alpha^{-1/2} \sup_{v_T^f \in V_{h,k,T}^f} \frac{\sum_{T \in \mathcal{T}_H} a_\mu(u_T^f, v_T^f) - a_\mu^T(u_H, v_T^f)}{(\sum_{T \in \mathcal{T}_H} \|v_T^f\|_1^2)^{1/2}} \\
&= \alpha^{-1/2} \rho^{-1/2} \underbrace{\sup_{v_T^f \in V_{h,k,T}^f} \frac{\mathfrak{B}_\mu(\mathbf{u}, (0, v_{T_1}^f, \dots, v_{T_{|\mathcal{T}_H|}}^f))}{\|(0, v_{T_1}^f, \dots, v_{T_{|\mathcal{T}_H|}}^f)\|_1}}_B.
\end{aligned}$$

Combining both estimates yields

$$\begin{aligned}
\|\mathbf{u}\|_{a,\mu}^2 &\leq 2\gamma_k^{-2}A^2 + (2\gamma_k^{-2}\alpha^{-1}\beta C_{k,\text{ovl}}\rho^{-1} + 2\alpha^{-1}C_{k,\text{ovl}}\rho^{-1} + \alpha^{-1})B^2 \\
&= 2\gamma_k^{-2}A^2 + \underbrace{(2\gamma_k^{-2} + 2\alpha^{-1}\kappa^{-1} + \alpha^{-1})}_{\leq 5\cdot\gamma_k^{-2}}B^2 \\
&\leq 5\cdot\gamma_k^{-2}(A^2 + B^2) \\
&= 5\cdot\gamma_k^{-2}\left(\sup_{\mathbf{v}\in\mathfrak{B}} \frac{\mathfrak{B}_\mu(\mathbf{u}, \mathbf{v})}{\|\mathbf{v}\|_1}\right)^2,
\end{aligned}$$

where we have used $\gamma_k \leq \alpha^{1/2}$ and $\kappa \geq 1$ in the third equality. In the last equality we have used the fact that the square norm of a linear functional on a direct sum of Hilbert spaces is the sum of the square norms of the functional restricted to the respective subspaces. \square

4.3 Error Bounds

Exploiting the inf-sup stability of \mathfrak{B}_μ , we now easily obtain error bounds w.r.t. the PG-LOD solution. We start with an a posteriori bound and define for arbitrary $\mathbf{u} \in \mathfrak{B}$ the residual-based error indicators

$$(14) \quad \eta_{a,\mu}(\mathbf{u}) := \sqrt{5}\gamma_k^{-1} \sup_{\mathbf{v}\in\mathfrak{B}} \frac{\mathfrak{F}(\mathbf{v}) - \mathfrak{B}_\mu(\mathbf{u}, \mathbf{v})}{\|\mathbf{v}\|_1},$$

$$(15) \quad \eta_{1,\mu}(\mathbf{u}) := \sqrt{5}C_{\mathcal{I}_H}\alpha^{-1/2}\gamma_k^{-1} \sup_{\mathbf{v}\in\mathfrak{B}} \frac{\mathfrak{F}(\mathbf{v}) - \mathfrak{B}_\mu(\mathbf{u}, \mathbf{v})}{\|\mathbf{v}\|_1}.$$

These error indicators provide strict and efficient upper bounds on the error between \mathbf{u} and the two-scale PG-LOD solution:

Theorem 4.7 (A posteriori bound). *Let $\mathbf{u} = (u_H, u_{T_1}^f, \dots, u_{T_{|\mathcal{T}_H|}}^f) \in \mathfrak{B}$ be an arbitrary two-scale function, denote by \mathbf{u}_μ the solution of the two-scale solution as in (12) for a given parameter μ , and let ρ be given as in Proposition 4.6. Then the following energy error bounds hold:*

$$(16) \quad \|\mathbf{u}_\mu - \mathbf{u}\|_{a,\mu} \leq \eta_{a,\mu}(\mathbf{u}) \leq \sqrt{5}\gamma_k^{-1}\beta^{1/2}\|\mathbf{u}_\mu - \mathbf{u}\|_{a,\mu}.$$

Further, we have

$$(17) \quad \left(\|u_{H,k,\mu} - u_H\|_1^2 + \rho \sum_{T \in \mathcal{T}_H} \|\mathcal{Q}_{k,\mu}^T(u_H) - u_T^f\|_1^2 \right)^{1/2} \leq \eta_{1,\mu}(\mathbf{u}),$$

and

$$(18) \quad \eta_{1,\mu}(\mathbf{u}) \leq \sqrt{15}C_{\mathcal{I}_H}(C_{k,\text{ovl}} + 1)^{1/2}\kappa^{1/2}\gamma_k^{-1}\beta^{1/2} \cdot \left(\|u_{H,k,\mu} - u_H\|_1^2 + \rho \sum_{T \in \mathcal{T}_H} \|\mathcal{Q}_{k,\mu}^T(u_H) - u_T^f\|_1^2 \right)^{1/2}.$$

Proof. Since \mathbf{u}_μ is a solution of (11) we have

$$\mathfrak{B}_\mu(\mathbf{u}_\mu - \mathbf{u}, \mathbf{v}) = \mathfrak{F}(\mathbf{v}) - \mathfrak{B}_\mu(\mathbf{u}, \mathbf{v}).$$

Hence, (16) directly follows from Proposition 4.6. Equations (17) and (18) follow from (16) using Proposition 4.5 and noting that for each $T \in \mathcal{T}_H$ we have

$$\|\mathcal{Q}_{k,\mu}^T(u_{H,k,\mu} - u_H) - (\mathcal{Q}_{k,\mu}^T(u_{H,k,\mu}) - u_T^f)\|_1 = \|\mathcal{Q}_{k,\mu}^T(u_H) - u_T^f\|_1.$$

\square

Finally, we also show a corresponding a priori result:

Theorem 4.8 (A priori bound). *Let $\bar{\mathfrak{V}}$ be an arbitrary linear subspace of \mathfrak{V} and let $\bar{\mathbf{u}}$ be the solution of the residual-minimization problem*

$$(19) \quad \bar{\mathbf{u}}_\mu := \operatorname{argmin}_{\mathbf{u} \in \bar{\mathfrak{V}}} \sup_{\mathbf{v} \in \mathfrak{V}} \frac{\mathfrak{F}(\mathbf{v}) - \mathfrak{B}_\mu(\mathbf{u}, \mathbf{v})}{\|\mathbf{v}\|_1},$$

then we have

$$\|\mathbf{u}_\mu - \bar{\mathbf{u}}_\mu\|_{a,\mu} \leq \sqrt{5} \gamma_k^{-1} \beta^{1/2} \min_{\bar{\mathbf{v}} \in \bar{\mathfrak{V}}} \|\mathbf{u}_\mu - \bar{\mathbf{v}}\|_{a,\mu},$$

and

$$\begin{aligned} & \left(\|u_{H,k,\mu} - u_H\|_1^2 + \rho \sum_{T \in \mathcal{T}_H} \|\mathcal{Q}_{k,\mu}^T(u_H) - u_T^f\|_1^2 \right)^{1/2} \\ & \leq \sqrt{15} C_{\mathcal{I}_H} (C_{k,ovl} + 1)^{1/2} \kappa^{1/2} \gamma_k^{-1} \beta^{1/2} \\ & \quad \cdot \min_{\bar{\mathbf{v}} \in \bar{\mathfrak{V}}} \left(\|u_{H,k,\mu} - \bar{v}_H\|_1^2 + \rho \sum_{T \in \mathcal{T}_H} \|\mathcal{Q}_{k,\mu}^T(u_H) - \bar{v}_T^f\|_1^2 \right)^{1/2}. \end{aligned}$$

Proof. This follows directly from Theorem 4.7 and the definition of $\bar{\mathbf{u}}_\mu$. \square

Note that for k large enough, we have $\gamma_k \approx \alpha^{1/2} C_{\mathcal{I}_H}^{-1}$ such that the a priori and a posteriori bounds have efficiencies of that scale with $\kappa^{1/2}$ in the energy norm and with κ in the 1-norm, which agrees with what is to be expected for these error bounds in a standard finite element setting.

5 Reduced Basis approach

In this section we describe the construction of the TSRBLOD ROM in detail. As with all RB methods, the ROM is defined by a projection of the original model equations, in our case the two-scale formulation (11), onto a reduced approximation space (subsection 5.2.1). Rigorous upper and lower bounds for the MOR error are given by a residual-based a posteriori error estimator (subsection 5.2.2). In order to be able to quickly assemble the ROM for a new parameter μ and to efficiently evaluate the error estimator, an offline-online decomposition of the ROM must be performed (subsection 5.2.3). As part of the offline phase, the reduced space is constructed as the linear span of FOM solutions \mathbf{u}_{μ^*} , where the snapshot parameters μ^* are selected via an iterative greedy search over \mathcal{P} (subsection 5.2.4).

The computation of the solution snapshots \mathbf{u}_{μ^*} via (12), however, requires for each new μ^* the recomputation of all corrector problems. For large problems this may be computationally infeasible. Thus, we combine our approach (Stage 2) with a preceding preparatory step similar to [6], where each corrector problem is replaced by an efficient ROM surrogate (Stage 1). These ROMs are then used in the offline phase of Stage 2 to compute approximate solution snapshots \mathbf{u}_{μ^*} . Again, Stage 1 is divided into ROM construction (subsection 5.1.1), error estimation (subsection 5.1.2), offline-online decomposition (subsection 5.1.3) and construction of the reduced spaces (subsection 5.1.4). After a Stage 1 ROM is constructed, all associated fine-mesh data can be deleted. In particular, all computations in Stage 2 are independent from size of \mathcal{T}_h .

We emphasize again that, compared to [6], the Stage 2 TSRBLOD ROM is not only independent from \mathcal{T}_h , but also from the number of coarse elements. Its size only depends on the number of selected basis vectors in subsection 5.2.4. Further, in contrast to [6], the derived error estimator fully takes the effect of the errors of the reduced corrector problems on the resulting global solution into account and, thus, rigorously bounds the error of the ROM w.r.t. the LOD solution.

5.1 Stage 1: Computing RB approximations of $\mathcal{Q}_{k,\mu}^T$ and $\mathbb{K}_{T,\mu}$

5.1.1 Definition of the reduced order model

Let $T \in \mathcal{T}_H$ be fixed, and let $V_{k,T}^{i,rb} \subset V_{h,k,T}^f$ be an approximation space for the correctors $\mathcal{Q}_{k,\mu}^T(v_H)$ of v_H for arbitrary $v_H \in V_H$ and $\mu \in \mathcal{P}$. Then, for given $v_H \in V_H$ and $\mu \in \mathcal{P}$, we determine an approximate corrector $\mathcal{Q}_{k,\mu}^{T,rb}(v_H) \in V_{k,T}^{i,rb}$ via Galerkin projection onto $V_{k,T}^{f,rb}$ as the solution of

$$(20) \quad a_\mu(\mathcal{Q}_{k,\mu}^{T,rb}(v_H), v_T^f) = a_\mu^T(v_H, v_T^f) \quad \forall v_T^f \in V_{k,T}^{f,rb}.$$

Note that $\mathcal{Q}_{k,\mu}^{T,rb}(v_H)$ is well-defined since a_μ is a coercive bilinear form. Using these reduced correction operators we can define an approximate localized multiscale matrix \mathbb{K}_μ^{rb} given by

$$\mathbb{K}_\mu^{rb} := \sum_{T \in \mathcal{T}_H} \mathbb{K}_{T,\mu}^{rb}, \quad (\mathbb{K}_{T,\mu}^{rb})_{j,i} := (A_\mu(\chi_T \nabla - \nabla \mathcal{Q}_{k,\mu}^{T,rb})\phi_i, \nabla \phi_j)_{U_k(T)}.$$

5.1.2 Error estimation

We employ standard RB tools for the a posteriori error estimation of the reduced system (20). In detail, we use the residual-norm based estimate:

$$(21) \quad \|\mathcal{Q}_{k,\mu}^T(v_H) - \mathcal{Q}_{k,\mu}^{T,rb}(v_H)\|_{a,\mu} \leq \eta_{T,\mu}(\mathcal{Q}_{k,\mu}^{T,rb}(v_H)) \leq \kappa^{1/2} \|\mathcal{Q}_{k,\mu}^T(v_H) - \mathcal{Q}_{k,\mu}^{T,rb}(v_H)\|_{a,\mu},$$

where

$$\eta_{T,\mu}(\mathcal{Q}_{k,\mu}^{T,rb}(v_H)) := \alpha^{-1/2} \sup_{v_T^f \in V_{h,k,T}^f} \frac{a_\mu^T(v_H, v_T^f) - a_\mu(\mathcal{Q}_{k,\mu}^{T,rb}(v_H), v_T^f)}{\|v_T^f\|_1}.$$

The bounds in (21) easily follow from the definition of $\mathcal{Q}_{k,\mu}^T(v_H)$ and the equivalence of $\|\cdot\|_{a,\mu}$ and $\|\cdot\|_1$.

5.1.3 Offline-Online Decomposition

In order to compute $\mathcal{Q}_{k,\mu}^{T,rb}(v_H)$ and subsequently $\mathbb{K}_{T,\mu}^{rb}$, let $N_T := \dim V_{k,T}^{f,rb}$, and choose a basis $\varphi_{T,n}$, $1 \leq n \leq N_T$, of $V_{k,T}^{f,rb}$. Expanding $\mathcal{Q}_{k,\mu}^{T,rb}(v_H)$ w.r.t. this basis as

$$\mathcal{Q}_{k,\mu}^{T,rb}(v_H) := \sum_{n=1}^{N_T} c_n \cdot \varphi_{T,n},$$

the coefficient vector $c \in \mathbb{R}^{N_T}$ is given as the solution of the $N_T \times N_T$ -dimensional linear system

$$(22) \quad \mathbb{A}_\mu^T \cdot c = \mathbb{G}_\mu^T(v_H),$$

where

$$(\mathbb{A}_\mu^T)_{m,n} := a_\mu(\varphi_{T,n}, \varphi_{T,m}) \quad \text{and} \quad \mathbb{G}_\mu^T(v_H)_m := a_\mu^T(v_H, \varphi_{T,m}).$$

While (22) can be solved quickly when N_T is sufficiently small, we still need to re-assemble this equation system for each new parameter μ and coarse-scale function v_H . This requires time and memory that scales with $\dim V_{h,k,T}^f$. To avoid these high-dimensional computations we exploit (4) and pre-assemble matrices and vectors

$$(\mathbb{A}_q^T)_{m,n} := a_q(\varphi_{T,n}, \varphi_{T,m}) \quad \text{and} \quad (\mathbb{G}_{q,j}^T)_m := a_q^T(\phi_{i_{T,j}}, \varphi_{T,m}),$$

for $1 \leq q \leq Q$ and $1 \leq j \leq J_T$, where J_T is the number of finite-element basis functions ϕ_i of V_H with support containing T and $i_{T,1}, \dots, i_{T,J_T}$ is an enumeration of these basis functions. Then, \mathbb{A}_μ^T and $\mathbb{G}_\mu^T(v_H)$ can be determined as

$$\mathbb{A}_\mu^T := \sum_{q=1}^Q \theta_q(\mu) \mathbb{A}_q^T \quad \text{and} \quad \mathbb{G}_\mu^T(v_H) := \sum_{q=1}^Q \sum_{j=1}^{J_T} \theta_q(\mu) \lambda_{i_{T,j}}(v_H) \mathbb{G}_{q,j}^T,$$

where by $\lambda_i \in V_H'$ we denote the dual basis of ϕ_i .

To compute \mathbb{K}_μ^{rb} , we further store the matrices

$$(\mathbb{K}_{T,q}^0)_{j,i} := (A_q \chi_T \nabla \phi_i, \nabla \phi_j)_{U_k(T)} \quad \text{and} \quad (\mathbb{K}_{T,q}^{rb})_{j,n} := (A_q \nabla \varphi_{T,n}, \nabla \phi_j)_{U_k(T)}.$$

Then we have:

$$(\mathbb{K}_{T,\mu}^{rb})_{j,i} = \sum_{q=1}^Q \theta_q(\mu) \left[(\mathbb{K}_{T,q}^0)_{j,i} - \sum_{n=0}^{N_T} c_n^i(\mu) (\mathbb{K}_{T,q}^{rb})_{j,n} \right],$$

where $c^i(\mu) \in \mathbb{R}^{N_T}$ is given as the solution of

$$\mathbb{A}_\mu^T \cdot c^i(\mu) = \mathbb{G}_\mu^T(\phi_i).$$

Note that $(\mathbb{K}_{q,0}^T)_{j,i}$, $(\mathbb{K}_q^T)_{j,n}$ and $c^i(\mu)$ are zero unless the support of ϕ_i is non-disjoint from T and the support of ϕ_j is non-disjoint from $U_k(T)$. In particular, only J_T reduced problems have to be solved in order to determine $\mathbb{K}_{T,\mu}^{rb}$. The total computational effort for solving these problems is of order $\mathcal{O}(QN_T^2 + N_T^3 + J_T N_T^2)$, where the first term corresponds to the assembly of \mathbb{A}_μ^T , the second term to its LU decomposition and third term to the solution of the J_T linear systems using forward/backward substitution.

Finally, to efficiently evaluate $\eta_{T,\mu}(\mathcal{Q}_{k,\mu}^{T,rb}(v_H))$, first note that

$$\eta_{T,\mu}(\mathcal{Q}_{k,\mu}^{T,rb}(v_H)) = \alpha^{-1/2} \|\mathcal{R}_{V_{h,k,T}^f}(a_\mu^T(v_H, \cdot) - a_\mu(\mathcal{Q}_{k,\mu}^{T,rb}(v_H), \cdot))\|_1,$$

where $\mathcal{R}_{V_{h,k,T}^f} : (V_{h,k,T}^f)' \rightarrow V_{h,k,T}^f$ denotes the Riesz isomorphism.

Following [12], let $W_{k,T}^{f,rb}$ denote the M_T -dimensional linear subspace of $V_{h,k,T}^f$ that is spanned by the vectors

$$\left\{ \mathcal{R}_{V_{h,k,T}^f}(a_q(\varphi_{T,n}, \cdot)) \mid 1 \leq q \leq Q, 1 \leq n \leq N_T \right\} \cup \left\{ \mathcal{R}_{V_{h,k,T}^f}(a_q^T(\phi_{i_{T,j}}, \cdot)) \mid 1 \leq q \leq Q, 1 \leq j \leq J_T \right\}.$$

Choose an H^1 -orthonormal basis $\psi_{T,m}$ of $W_{k,T}^{f,rb}$. Since $\mathcal{R}_{V_{h,k,T}^f}(a_\mu^T(v_H, \cdot) - a_\mu(u_N, \cdot))$ lies in $W_{k,T}^{f,rb}$ for each $u_N \in V_{k,T}^{f,rb}$, we obtain

$$\begin{aligned} \eta_{T,\mu}(\mathcal{Q}_{k,\mu}^{T,rb}(v_H)) &= \alpha^{-1/2} \left\| \left[\left(\mathcal{R}_{V_{h,k,T}^f}(a_\mu^T(v_H, \cdot) - a_\mu(\mathcal{Q}_{k,\mu}^{T,rb}(v_H), \cdot)), \psi_{T,m} \right) \right]_{m=1}^{M_T} \right\| \\ &= \alpha^{-1/2} \left\| \left[a_\mu^T(v_H, \psi_{T,m}) - a_\mu(\mathcal{Q}_{k,\mu}^{T,rb}(v_H), \psi_{T,m}) \right]_{m=1}^{M_T} \right\|. \end{aligned}$$

Hence, defining the M_T -dimensional vectors and $M_T \times N_T$ matrices

$$(23) \quad (\hat{\mathbb{G}}_{q,j}^T)_m := a_q^T(\phi_{i_{T,j}}, \psi_{T,m}) \quad \text{and} \quad (\hat{\mathbb{A}}_q^T)_{m,n} := a_q(\varphi_{T,n}, \psi_{T,m}),$$

we obtain

$$(24) \quad \eta_{T,\mu}(\mathcal{Q}_{k,\mu}^{T,rb}(v_H)) = \alpha^{-1/2} \left\| \sum_{q=1}^Q \theta_q(\mu) \left(\sum_{j=1}^{J_T} \lambda_{i_{T,j}}(v_H) \hat{\mathbb{G}}_{q,j}^T - \hat{\mathbb{A}}_q^T \cdot c \right) \right\|,$$

where c is again given by (22). We remark that M_T can be bounded by $Q(N_T + J_T)$. Hence, the cost of evaluating (24) is of order $\mathcal{O}(Q^2(N_T + J_T)^2)$.

5.1.4 Basis generation

To build the reduced spaces $V_{k,T}^{f,rb}$, we use a standard weak greedy [10] approach in order to minimize the model order reduction error $\mathcal{Q}_{k,\mu}^T(v_H) - \mathcal{Q}_{k,\mu}^{T,rb}(v_H)$ for all $\mu \in \mathcal{P}$ and $v_H \in V_H$. To this end, we choose a target error tolerance ε_1 and an appropriate training set of parameters $\mathcal{P}_{\text{train}}$, over which we estimate the maximum reduction error. The initial reduced space $V_{k,T}^{f,rb}$ is chosen as the zero-dimensional space. Then, in each iteration, the reduction error is estimated with $\eta_{T,\mu}(\mathcal{Q}_{k,\mu}^{T,rb}(v_H))$ for all $\mu \in \mathcal{P}_{\text{train}}$ and $\phi_{i_{T,j}}$, and a pair μ^* , $\phi_{i_{T,j^*}}$ maximising the estimate is selected. Thanks to the offline-online decomposition of $\eta_{T,\mu}$ this step does not involve any high-dimensional computations, so $\mathcal{P}_{\text{train}}$ can be chosen large. Since (20) is linear, it suffices to consider the basis functions $\phi_{i_{T,j}}$ as v_H . After μ^* , j^* have been found, $\mathcal{Q}_{k,\mu^*}^{T,rb}(\phi_{i_{T,j^*}})$ is computed. $V_{k,T}^{f,rb}$ is extended with this solution *snapshot*, and the offline-online decomposition for this extended reduced space is computed. The iteration ends, when the maximum estimated error drops below ε_1 . A formal definition of the procedure is given in Algorithm 1.

Algorithm 1: Weak greedy algorithm for the generation of $V_{k,T}^{f,rb}$.

Data: $T, \mathcal{P}_{\text{train}}, \varepsilon_1$
Result: $V_{k,T}^{f,rb}$

- 1 $V_{k,T}^{f,rb} \leftarrow \{0\};$
- 2 **while** $\max_{\mu \in \mathcal{P}_{\text{train}}} \max_{1 \leq j \leq J_T} \eta_{T,\mu}(\mathcal{Q}_{k,\mu}^{T,rb}(\phi_{i_T,j})) > \varepsilon_1$ **do**
- 3 $(\mu^*, j^*) \leftarrow \arg \max_{(\mu^*, j^*) \in \mathcal{P}_{\text{train}} \times \{1, \dots, J_T\}} \eta_{T,\mu}(\mathcal{Q}_{k,\mu}^{T,rb}(\phi_{i_T,j}));$
- 4 $V_{k,T}^{f,rb} \leftarrow \text{span}(V_{k,T}^{f,rb} \cup \{\mathcal{Q}_{k,\mu^*}^T(\phi_{i_T,j^*})\});$
- 5 **end**

5.2 Stage 2: Computing RB approximations of \mathbf{u}_μ

5.2.1 Definition of the reduced order model

In order to find an approximate solution of \mathbf{u}_μ , we assume to be given an appropriate reduced subspace \mathfrak{V}^{rb} of \mathfrak{V} . As we have proven inf-sup stability of \mathfrak{B}_μ in Proposition 4.6, and since the inf-sup stability is preserved by restricting \mathfrak{B}_μ to a linear subspace, we can define the reduced two-scale solution \mathbf{u}_μ^{rb} as the unique solution of the residual minimization problem

$$(25) \quad \mathbf{u}_\mu^{rb} := \operatorname{argmin}_{\mathbf{u} \in \mathfrak{V}^{rb}} \sup_{\mathbf{v} \in \mathfrak{V}} \frac{\mathfrak{F}(\mathbf{v}) - \mathfrak{B}_\mu(\mathbf{u}, \mathbf{v})}{\|\mathbf{v}\|_1}.$$

As a direct consequence of Theorem 4.8, \mathbf{u}_μ^{rb} is a quasi best-approximation of \mathbf{u}_μ within \mathfrak{V}^{rb} .

5.2.2 Error estimation

We have already defined a posteriori error estimators for approximations of the two-scale solution \mathbf{u}_μ in subsection 4.3. In Theorem 4.7 we have shown that these estimators yield efficient upper bounds for the approximation errors in the two-scale energy norm as well as in the Sobolev 1-norm. Note that even though we will use the Stage 1 approximations $\mathbb{K}_{T,\mu}^{rb}$ of $\mathbb{K}_{T,\mu}$ to build the reduced space \mathfrak{V}^{rb} , the derived error estimates are with respect to the true LOD solution and take these approximation errors into account.

5.2.3 Offline-Online Decomposition

For the offline-online decomposition of (25), we proceed similar to the decomposition of the Stage 1 error estimator $\eta_{T,\mu}$. Denote by $\mathcal{R}_{\mathfrak{V}} : \mathfrak{V}' \rightarrow \mathfrak{V}$ the Riesz isomorphism for \mathfrak{V} . Then (25) is equivalent to solving

$$(26) \quad \mathbf{u}_\mu^{rb} := \operatorname{argmin}_{\mathbf{u} \in \mathfrak{V}^{rb}} \|\mathcal{R}_{\mathfrak{V}}(\mathfrak{F}) - \mathcal{R}_{\mathfrak{V}}(\mathfrak{B}_\mu(\mathbf{u}, \cdot))\|_1^2.$$

Let $N := \dim \mathfrak{V}^{rb}$, and let \mathbf{b}_n , $1 \leq n \leq N$ be a basis of \mathfrak{V}^{rb} . We again construct an $\|\cdot\|_1$ -orthonormal basis \mathbf{c}_m for the M -dimensional subspace \mathfrak{W}^{rb} of \mathfrak{V} spanned by the vectors

$$(27) \quad \{\mathcal{R}_{\mathfrak{V}}(\mathfrak{F})\} \cup \{\mathcal{R}_{\mathfrak{V}}(\mathfrak{B}_q(\mathbf{b}_n, \cdot)) \mid 1 \leq n \leq N, 1 \leq q \leq Q\},$$

where

$$\mathfrak{B}_q \left((u_H, u_{T_1}^f, \dots, u_{T_{|\mathcal{T}_H|}}^f), (v_H, v_{T_1}^f, \dots, v_{T_{|\mathcal{T}_H|}}^f) \right) := a_q(u_H - \sum_{T \in \mathcal{T}_H} u_T^f, v_H) + \rho^{1/2} \sum_{T \in \mathcal{T}_H} a_q(u_T^f, v_T^f) - a_q^T(u_H, v_T^f),$$

such that \mathfrak{B}_μ has the decomposition: $\mathfrak{B}_\mu = \sum_{q=1}^Q \theta_q(\mu) \mathfrak{B}_q$. Using these bases, we define matrices $\hat{\mathbb{A}}_q \in \mathbb{R}^{M \times N}$ and the vector $\hat{\mathbb{F}} \in \mathbb{R}^M$ by

$$(\hat{\mathbb{A}}_q)_{m,n} := \mathfrak{B}_q(\mathbf{b}_n, \mathbf{c}_m) \quad \text{and} \quad \hat{\mathbb{F}}_m := \mathfrak{F}(\mathbf{c}_m).$$

Then, with $\hat{\mathbb{A}}_\mu := \sum_{q=1}^Q \theta_q(\mu) \hat{\mathbb{A}}_q$, solving (26) is equivalent to solving the least-squares problem

$$(28) \quad c(\mu) := \operatorname{argmin}_{c \in \mathbb{R}^N} \|\hat{\mathbb{F}} - \hat{\mathbb{A}}_\mu \cdot c\|^2,$$

where $\mathbf{u}_\mu = \sum_{n=1}^N c_n(\mu) \mathbf{b}_n$. In the same way we can evaluate the error bounds $\eta_{a,\mu}(\mathbf{u}_\mu)$ and $\eta_{1,\mu}(\mathbf{u})$ as

$$\begin{aligned} \eta_{a,\mu}(\mathbf{u}_\mu) &= \sqrt{5} \gamma_k^{-1} \|\hat{\mathbb{F}} - \hat{\mathbb{A}}_\mu \cdot c(\mu)\|, \\ \eta_{1,\mu}(\mathbf{u}_\mu) &= \sqrt{5} C_{\mathcal{I}_H} \alpha^{-1/2} \gamma_k^{-1} \|\hat{\mathbb{F}} - \hat{\mathbb{A}}_\mu \cdot c(\mu)\|. \end{aligned}$$

Since $M \leq QN + 1$, the computational effort for assembling the least-squares system is of order $\mathcal{O}(Q^2 N^2)$. Solving the system requires $\mathcal{O}(QN^3)$ operations, and evaluating the estimators requires $\mathcal{O}(Q^2 N^2)$ operations. In particular, the computational effort is completely independent from h and H .

We still need to show how the matrices $\hat{\mathbb{A}}_q$ and the vector $\hat{\mathbb{F}}$ can be computed after Stage 1 without using any data or operations associated with the fine mesh \mathcal{T}_h . To this end, we assume that $\mathfrak{V}^{rb} \subseteq V_H \oplus V_{k,T_1}^{f,rb} \oplus \dots \oplus V_{k,T_{|\mathcal{T}_H|}}^{f,rb} \subset \mathfrak{V}$. By construction of the $W_{k,T}^{f,rb}$, we see that for such a \mathfrak{V}^{rb} , \mathfrak{W}^{rb} is a linear subspace of $V_H \oplus W_{k,T_1}^{f,rb} \oplus \dots \oplus W_{k,T_{|\mathcal{T}_H|}}^{f,rb}$. Choose a basis \mathbf{b}_n of \mathfrak{V}^{rb} with coefficient vectors

$$\underline{\mathbf{b}}_n = (\underline{\mathbf{b}}_{n,H}, \underline{\mathbf{b}}_{n,T_1}, \dots, \underline{\mathbf{b}}_{n,T_{|\mathcal{T}_H|}}) \in \mathbb{R}^{N_H} \oplus \mathbb{R}^{M_{T_1}} \oplus \dots \oplus \mathbb{R}^{M_{T_{|\mathcal{T}_H|}}}$$

w.r.t. the finite element basis ϕ_i of V_H and the reduced bases $\varphi_{T,n}$ of $V_{k,T}^{f,rb}$. Denote by \mathbb{S} the $N_H \times N_H$ matrix of the Sobolev 1-inner product on V_H given by

$$\mathbb{S}_{j,i} := \int_{\Omega} \nabla \phi_i \cdot \nabla \phi_j \, dx,$$

and use the H^1 -orthonormal bases $\psi_{T,m}$ to isometrically represent the vectors (27) as coefficient vectors in the direct sum Hilbert space $\underline{\mathfrak{W}}^{rb} := \mathbb{R}^{N_H} \oplus \mathbb{R}^{M_{T_1}} \oplus \dots \oplus \mathbb{R}^{M_{T_{|\mathcal{T}_H|}}$ equipped with the \mathbb{S} -inner product in the first and with the Euclidean inner products in the remaining components. Checking the definitions of \mathfrak{B}_q , \mathfrak{F} , $\hat{\mathbb{A}}_q^T$, $\hat{\mathbb{G}}_{q,j}^T$, $\mathbb{K}_{T,q}^0$ and $\mathbb{K}_{T,q}^{rb}$, we obtain the vectors

$$(29) \quad (\mathbb{S}^{-1} \cdot [F(\phi_i)]_i, 0, \dots, 0),$$

and

$$(30) \quad \begin{pmatrix} \mathbb{S}^{-1} \cdot \sum_{T \in \mathcal{T}_H} (\mathbb{K}_{T,q}^0 \cdot \underline{\mathbf{b}}_{n,H} - \mathbb{K}_{T,q}^{rb} \cdot \underline{\mathbf{b}}_{n,T}) \\ \rho^{1/2} \hat{\mathbb{A}}_q^T \underline{\mathbf{b}}_{n,T_1} - \rho^{1/2} \sum_{j=1}^{J_{T_1}} \underline{\mathbf{b}}_{n,H,i_{T_1,j}} \hat{\mathbb{G}}_{q,j}^{T_1} \\ \vdots \\ \rho^{1/2} \hat{\mathbb{A}}_q^T \underline{\mathbf{b}}_{n,T_{|\mathcal{T}_H|}} - \rho^{1/2} \sum_{j=1}^{J_{T_{|\mathcal{T}_H|}}} \underline{\mathbf{b}}_{n,H,i_{T_{|\mathcal{T}_H|},j}} \hat{\mathbb{G}}_{q,j}^{T_{|\mathcal{T}_H|}} \end{pmatrix},$$

for $1 \leq n \leq N$. After having computed (29) and (30), we compute a $\underline{\mathfrak{W}}^{rb}$ -orthonormal basis $\underline{\mathbf{c}}_m$ for these vectors with coefficients

$$\underline{\mathbf{c}}_m = (\underline{\mathbf{c}}_{m,H}, \underline{\mathbf{c}}_{m,T_1}, \dots, \underline{\mathbf{c}}_{m,T_{|\mathcal{T}_H|}}),$$

such that

$$\underline{\mathbf{c}}_m := \left(\sum_{i=1}^{N_H} \underline{\mathbf{c}}_{m,H,i} \cdot \phi_i, \sum_{l=1}^{M_{T_1}} \underline{\mathbf{c}}_{m,T_1,l} \cdot \psi_{T,l}, \dots, \sum_{l=1}^{M_{T_{|\mathcal{T}_H|}}} \underline{\mathbf{c}}_{m,T_{|\mathcal{T}_H|},l} \cdot \psi_{T,l} \right)$$

is an $\|\cdot\|_1$ -orthonormal orthonormal basis for $\underline{\mathfrak{W}}^{rb}$.

Finally, following the definitions again, we see that $\hat{\mathbb{A}}_q$ and $\hat{\mathbb{F}}$ can be computed as

$$\hat{\mathbb{F}}_m = \mathcal{F}(\underline{\mathbf{c}}_m) = \sum_{i=1}^{N_H} \underline{\mathbf{c}}_{m,H,i} \cdot F(\phi_i),$$

and

$$\begin{aligned}
(\hat{\mathbb{A}}_q)_{m,n} &= \mathfrak{B}_q(\mathbf{b}_n, \mathbf{c}_m) \\
&= \sum_{T \in \mathcal{T}_H} \boldsymbol{\xi}_{m,H}^T \cdot (\mathbb{K}_{T,q}^0 \cdot \mathbf{b}_{n,H} - \mathbb{K}_{T,q}^{rb} \cdot \mathbf{b}_{n,T}) \\
&\quad + \rho^{1/2} \sum_{T \in \mathcal{T}_H} \left((\boldsymbol{\xi}_{m,T})^T \cdot \hat{\mathbb{A}}_q^T \cdot \mathbf{b}_{n,T} - \sum_{j=1}^{J_{T|\mathcal{T}_H|}} (\boldsymbol{\xi}_{m,T})^T \cdot \hat{\mathbb{G}}_{q,j}^T \cdot \mathbf{b}_{n,H,i_{T,j}} \right).
\end{aligned}$$

5.2.4 Basis generation

To build the reduced Stage 2 space \mathfrak{V}^{rb} , we follow the same methodology as in subsection 5.1.4 and use a greedy search procedure to iteratively extend \mathfrak{V}^{rb} until a given error tolerance ε_2 for the MOR error estimate $\eta_{a,\mu}(\mathbf{u}_\mu^{rb})$ is reached. However, in contrast to subsection 5.1.4, we will not use the full-order model (11), or equivalently (10), to compute solution snapshots, but rather its Stage 1 approximation. I.e., we solve

$$(31) \quad \mathbb{K}_\mu^{rb} \cdot \mathbf{u}_{H,k,\mu} = \mathbb{F}$$

to determine the V_H -component of the solution, followed by solving the Stage 1 corrector ROMs (20) for each $T \in \mathcal{T}_H$ to determine the fine-scale components $\mathcal{Q}_{k,\mu}^{T,rb}(\mathbf{u}_{H,k,\mu})$ of the two-scale solution snapshot. The full algorithm is given by Algorithm 2.

Since we only extend \mathfrak{V}^{rb} with approximations of the true solution snapshots of the full-order model, note that Algorithm 2 is no longer a weak greedy algorithm in the sense of [10]. In particular note that the model reduction error is generally non-zero even for parameters μ^* for which the corresponding Stage 1 snapshot has been added to \mathfrak{V}^{rb} . Thus, when ε_1 is chosen too large in comparison to ε_2 , a single μ^* might be selected twice, causing Algorithm 2 to fail. In such a case, the individual Stage 1 errors for each $T \in \mathcal{T}_H$ can be estimated to further enrich the Stage 1 spaces for which the error is too large. We will not discuss such an approach in more detail here and instead note that in practice it is feasible to choose ε_1 small enough to avoid such issues (cf. section 6). In particular, for sufficiently small ε_1 we can expect the convergence rates of a weak greedy algorithm with exact solution snapshots to be preserved by Algorithm 2 up to the given target tolerance ε_2 .

Algorithm 2: Weak greedy algorithm for the generation of \mathfrak{V}^{rb} .

Data: $\mathcal{P}_{\text{train}}, \varepsilon_2$
Result: \mathfrak{V}^{rb}

- 1 $\mathfrak{V}^{rb} \leftarrow \{0\};$
- 2 **while** $\max_{\mu \in \mathcal{P}_{\text{train}}} \eta_{a,\mu}(\mathbf{u}_\mu^{rb}) > \varepsilon_2$ **do**
- 3 $\mu^* \leftarrow \arg \max_{\mu \in \mathcal{P}_{\text{train}}} \eta_{a,\mu}(\mathbf{u}_\mu^{rb});$
- 4 $\mathbf{u}_{H,k,\mu^*} \leftarrow$ solution of (31);
- 5 $\mathfrak{V}^{rb} \leftarrow \text{span}(\mathfrak{V}^{rb} \cup \{(\mathbf{u}_{H,k,\mu^*}, \mathcal{Q}_{k,\mu^*}^{T_1,rb}(\mathbf{u}_{H,k,\mu^*}), \dots, \mathcal{Q}_{k,\mu^*}^{T_{|\mathcal{T}_H|},rb}(\mathbf{u}_{H,k,\mu^*}))\});$
- 6 **end**

6 Numerical experiments

In this section we apply the above described method to two test cases and evaluate its efficiency. For the first, smaller problem we mainly investigate the MOR error and the performance of the certified error estimator. The second, large-scale problem will be used to assess the computational speed-up achieved by the TSRBLOD.

In both cases, we use structured 2D-grids $\mathcal{T}_h, \mathcal{T}_H$ with quadrilateral elements on the domain $\Omega = [0, 1]^2$. We specify the number of elements by $n_h \times n_h$ and $n_H \times n_H$ respectively. We use the interpolation operator from [29, Example 3.1] and choose the oversampling parameter k as the first integer to satisfy $k > |\log(H)|$. For the evaluation of the error estimator $\eta_{a,\mu}$ (14) we

approximate $\gamma_k \approx \alpha^{1/2} C_{T_H}^{-1}$ and assume $C_{T_H} \approx 1$. For quadrilateral elements, the overlapping constant can be explicitly computed by $C_{k,\text{ovl}} = (2k + 1)^2$. Moreover, we approximate α and the contrast κ by replacing \mathcal{P} in (2) by the training set $\mathcal{P}_{\text{train}}$. Thus, while it is not guaranteed that our approximations yield strict upper bounds on the model order reduction error, the decay rate and choice of snapshot parameters will not be affected.

We use an MPI distributed implementation to benefit from parallelization of the localized corrector problems, which gives significant speed-ups for all considered methods. All our computations have been performed on an HPC cluster with 1024 parallel processes.

Petrov–Galerkin variant of the RBLD method In order to compare our method to the RBLD approach introduced in [6], we have implemented a corresponding version of the RBLD that is applicable to our LOD formulation. In particular, we use the interpolation operator from [29, Example 3.1] and Petrov-Galerkin projection (7) in contrast to the Clément interpolation and Galerkin projection used in [6]. Further, in [6] individual ROMs for the local correctors $\mathcal{Q}_{k,\mu}^T(\phi_i)$ are constructed, where the snapshot parameters are chosen identically among all $\mathcal{Q}_{k,\mu}^{T'}(\phi_i)$, $T' \subset \text{supp } \psi_z$. In the RBLD variant implemented by us, we independently train the corrector ROMs for each $T \in \mathcal{T}_H$ as is done in Stage 1 of the TSRBLD. We note that for both RBLD variants, the number of ROMs constructed for each coarse element T is equal to the number of coarse-mesh basis functions ϕ_i supported on this element, whereas Stage 1 of the TSRBLD constructs a single ROM to approximate all local correctors.

Error measures To quantify the accuracy of the TSRBLD, we use a validation set $\mathcal{P}_{\text{val}} \subset \mathcal{P}$ of 10 random parameters and compute the maximum relative approximation errors w.r.t. the PG–LOD solutions for this set, i.e.,

$$e_{\text{LOD}}^{*,\text{rel}} := \max_{\mu \in \mathcal{P}_{\text{val}}} \frac{\|u_{H,k,\mu} - \tilde{u}_\mu\|_*}{\|u_{H,k,\mu}\|_*},$$

where \tilde{u}_μ denotes the coarse-scale component of either the RBLD or TSRBLD solution, $u_{H,k,\mu}$ denotes the coarse component of the PG–LOD solution (7), and $*$ stands for either the H^1 - or L^2 -norm. With the solution of the FEM approximation $u_{h,\mu}$ w.r.t. \mathcal{T}_h , we let

$$e_{\text{FEM}}^{L^2,\text{rel}} := \max_{\mu \in \mathcal{P}_{\text{val}}} \frac{\|u_{h,\mu} - \tilde{u}_\mu\|_{L^2}}{\|u_{h,\mu}\|_{L^2}}, \quad e_{\text{LOD-FEM}}^{L^2,\text{rel}} := \max_{\mu \in \mathcal{P}_{\text{val}}} \frac{\|u_{h,\mu} - u_{H,k,\mu}\|_{L^2}}{\|u_{h,\mu}\|_{L^2}}.$$

Time measures For an analysis of the computational wall times, we consider the following quantities:

- $t_{1,\text{av}}^{\text{offline}}(T)$: Average (arithmetic mean) time for creating a ROM for the localized corrector problem(s) corresponding to a single coarse element $T \in \mathcal{T}_H$ as discussed in subsection 5.1. For the RBLD, this involves all individual corrector problems for the four basis functions that are supported on T .
- t_1^{offline} : Total time required to build the corrector ROMs. In case of full parallelization, this is equal to the maximum of the Stage 1 times over all $T \in \mathcal{T}_H$.
- t_2^{offline} : Time for creating the Stage 2 TSRBLD ROM as discussed in subsection 5.2.
- t^{offline} : Total offline time for building the final reduced model. For the RBLD this is equal to t_1^{offline} . For the TSRBLD this additionally includes t_2^{offline} .
- t^{online} : Average time for solving the obtained ROM for a single new $\mu \in \mathcal{P}_{\text{val}}$. In case of the RBLD, the reduced corrector problems are solved sequentially on a single compute node.
- t^{LOD} : Average time needed to compute the PG–LOD with parallelization of the corrector problems for a single new $\mu \in \mathcal{P}_{\text{val}}$.

mesh size n_H	2^3		2^4		2^5	
method	RBLOD	TSRBLOD	RBLOD	TSRBLOD	RBLOD	TSRBLOD
$t_{1,\text{av}}^{\text{offline}}(T)$	41	61	39	61	33	55
t_1^{offline}	71	106	67	102	63	98
t_2^{offline}	-	8	-	56	-	472
t^{offline}	71	114	67	158	63	570
cum. size St.1	2346	1670	8718	6134	31810	22189
av. size St.1	9.16	26.09	8.51	23.96	7.77	21.67
size St.2	-	8	-	9		9
t_{LOD}	0.69		0.49		0.90	
t_{online}	0.0610	0.0003	0.2272	0.0003	1.0462	0.0003
speed-up LOD	11	2506	2	1536	1	2714
$e_{\text{LOD}}^{H^1,\text{rel}}$	1.97e-5	7.30e-4	5.08e-5	2.94e-4	1.11e-4	4.21e-4
$e_{\text{LOD}}^{L^2,\text{rel}}$	4.89e-6	2.71e-4	6.77e-6	1.03e-4	7.70e-6	1.32e-4
$e_{\text{FEM}}^{L^2,\text{rel}}$	2.46e-2	2.46e-2	9.05e-3	9.05e-3	3.98e-3	3.98e-3
$e_{\text{LOD-FEM}}^{L^2,\text{rel}}$	2.46e-2		9.05e-3		3.98e-3	

Table 1: Performance, ROM sizes and accuracy of the methods for test case 1 with tolerances $\varepsilon_1 = 0.001$ and $\varepsilon_2 = 0.01$ and varying coarse-mesh sizes. All times are given in seconds.

6.1 Test case 1

The first test case is taken from [6, Section 4.1] and has a one-dimensional parameter space $\mathcal{P} := [0, 5]$. The coefficient A_μ is visualized in Figure 1, and we set $f \equiv 1$. For the sake of brevity, we refer to [6] for an exact definition of A_μ . In order to resolve the microstructure of the problem, we choose $n_h = 2^8$ which results in 65, 536 fine-scale elements. The approximated maximum contrast of A_μ is $\kappa \approx 13$.

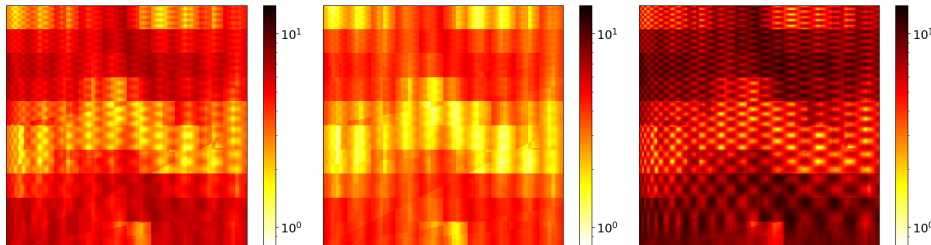


Figure 1: Diffusion coefficient A_μ for $\mu_1 = 1.8727$ (left), $\mu_2 = 2.904$ (middle), and $\mu_3 = 4.7536$ (right) for test case 1.

6.1.1 Performance and error comparison

We vary the coarse mesh size, $n_H \in \{2^3, 2^4, 2^5\}$, and show results for $\varepsilon_1 = 0.001$, $\varepsilon_2 = 0.01$ and a training set $\mathcal{P}_{\text{train}} \subset \mathcal{P}$ of 50 equidistant parameters in Table 1.

We observe that this choice of tolerances clearly suffices for both the RBLOD and TSRBLOD to match the error of the PG-LOD solution w.r.t. the FEM reference solution. For all coarse mesh sizes, the TSRBLOD produces a ROM with 8 or 9 basis functions without losing accuracy. The offline phase of Stage 1 for the TSRBLOD is longer and yields larger ROMs per element than the RBLOD. However, for the RBLOD four ROMs per element are required s.t. the total number of basis vectors actually is smaller for the TSRBLOD. The offline time for Stage 2 increases for larger n_H due to the increasing complexity of assembling and solving the coarse-scale problem, even with

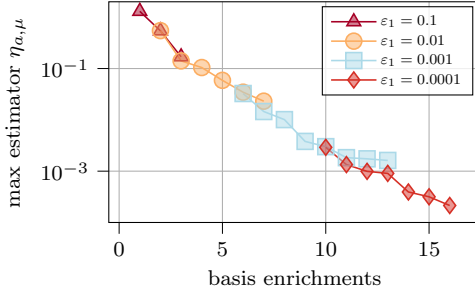


Figure 2: Evolution of the maximum estimated error $\eta_{a,\mu}$, $\mu \in \mathcal{P}_{\text{train}}$ for different Stage 1 tolerances ε_1 during the greedy algorithm of Stage 2 ($n_H = 2^4$). The greedy algorithm has been continued until the enrichment failed. The first values for smaller tolerances are left out to improve readability.

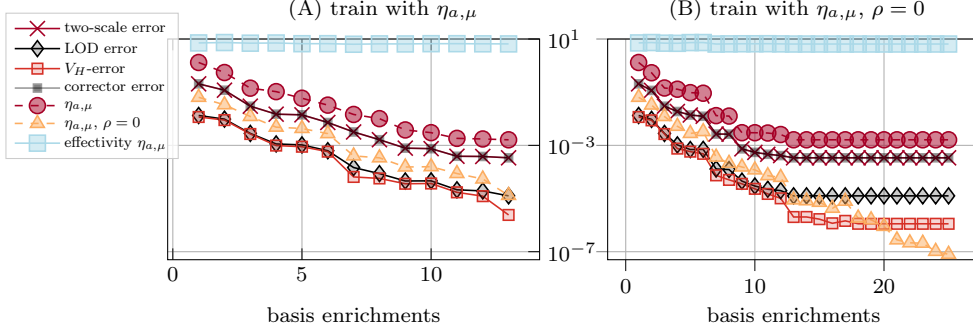


Figure 3: Comparison of the Stage 2 training error decay using different error estimators ($\varepsilon_1 = 0.001$). The greedy algorithm is continued until the enrichment fails or 25 enrichments are reached. Depicted is the maximum value of the full two-scale error $\|\mathbf{u}_\mu - \mathbf{u}_\mu^{\text{rb}}\|_{a,\mu}$, the LOD error given by $\|\mathbf{u}_\mu - \mathbf{u}_\mu^{\text{rb}}\|_{a,\mu}$ with $\rho = 0$, the V_H -error $\|u_{H,k,\mu} - u_{H,k,\mu}^{\text{rb}}\|_{a,\mu}$, the fine-scale corrector error $\rho^{1/2} \cdot (\sum_{T \in \mathcal{T}_H} \|\mathcal{Q}_{k,\mu}^T(u_{H,k,\mu}^{\text{rb}} - u_T^{\text{rb},f})\|_{a,\mu}^2)^{1/2}$, the estimator $\eta_{a,\mu}$, its effectivity $\eta_{a,\mu}/\|\mathbf{u}_\mu - \mathbf{u}_\mu^{\text{rb}}\|_{a,\mu}$ and the part of $\eta_{a,\mu}$ corresponding to the LOD residual (obtained by setting $\rho = 0$). The maximum is computed over the training set $\mathcal{P}_{\text{train}}$. The error estimator used in the greedy algorithm is either (A) the two-scale error estimator $\eta_{a,\mu}$ or (B) only its LOD-residual part ($\rho = 0$).

an RB approximation of the corrector problems. However, this only effects the offline phase for the TSRBLOD, and the online times stay at a constant level since the dimension of the Stage 2 ROM is largely unaffected by the number of coarse elements. Considering the speed-ups achieved by both methods, it can clearly be seen that the RBLOD has just a slight benefit over the (parallelized) PG-LOD, whereas the TSRBLOD shows a significant speed-up for all n_H without requiring any parallelization.

6.1.2 Error and estimator decay

Next we study the influence of the Stage 1 tolerance ε_1 on the training of the Stage 2 ROM. To this end, we fix the number of coarse mesh elements $n_H = 2^4$ and depict in Figure 2 for different ε_1 the maximum estimated training error w.r.t. the number of basis functions of the Stage 2 ROM. For all ε_1 , the Stage 2 training was continued until enrichment failed due to repeated selection of the same snapshot parameter (cf. subsection 5.2.4). As expected, a sufficiently small ε_1 is required to achieve small errors for the Stage 2 ROM. Note, however, that choosing a smaller ε_1 for the same ε_2 only affects the offline time of the Stage 2 training, but not the efficiency of the resulting Stage 2 ROM.

In Figure 3(A), we study in more detail how the two-scale error $\|\mathbf{u}_\mu - \mathbf{u}_\mu^{\text{rb}}\|_{a,\mu}$ and its estimator $\eta_{a,\mu}$ are affected by the coarse- and fine-scale errors in the two-scale system. We observe that the greedy algorithm aborts when the error in the fine-scale correctors stagnates at the lower bound determined by the fixed Stage 1 ROMs which are used to generate the Stage 2 solution snapshots. While the LOD error ($\|\cdot\|_{a,\mu}$ with $\rho = 0$) and the corresponding residual norms ($\eta_{a,\mu}$ with $\rho = 0$) decrease over all iterations, the corrector residuals dominate $\eta_{a,\mu}$, finally causing the same snapshot parameter to be selected twice.

To verify that the enrichment procedure should, indeed, be stopped at this point, we perform

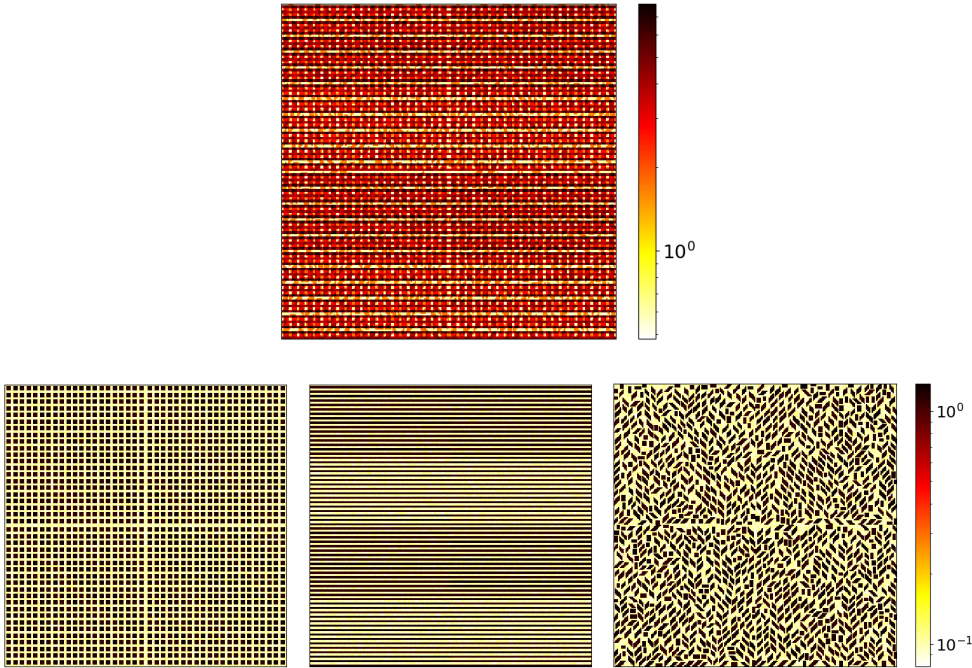


Figure 4: Coefficient A_μ on 4 of 4096 coarse elements for $\mu = (1, 2, 3)^T$ (top center) and A_q for all $q = 1, 2, 3$ (bottom from left to right). All coefficients A_q are subjected to normally distributed noise in the interval $[1, 1.2]$ for the particles (black) and in the interval $[0.03, 0.11]$ for the background (yellow). To ensure reproducibility, for every coarse-mesh element T , we choose the random seed for the noise and for the distribution of the randomly shaped particles in A_3 as the global index of T in \mathcal{T}_H .

another experiment where we neglect the corrector residuals and use $\eta_{a,\mu}$ with $\rho = 0$ as the error surrogate in the greedy algorithm. This corresponds to treating the RBLOD coarse system as the FOM w.r.t. which the MOR error is estimated. The result is visualized in Figure 3(B). We see that, while the estimator rapidly decays over all 25 enrichments, both the two-scale and LOD errors do not decrease any further. This is expected as both error measures involve the error in the fine-scale correctors. However, also the V_H -error $\|u_{H,k,\mu} - u_{H,k,\mu}^{\text{rb}}\|_{a,\mu}$ stagnates after one further iteration, and the estimator eventually underestimates all three errors. This underlines that the fine-scale corrector errors need to be taken into account, even if one is only interested in a coarse-scale approximation in V_H .

6.2 Test case 2

We now consider a more complex test case with significantly larger fine-scale mesh \mathcal{T}_h . The three-dimensional parameter space is given by $\mathcal{P} := [1, 5]^3$, and we let $A_\mu := \sum_{q=1}^3 \mu_q A_q$, where for a representative patch of four coarse-mesh elements the randomly generated functions A_q are given according to Figure 4, and we again set $f \equiv 1$. The exact definition of the functions A_q can be found in the accompanying code. The approximate maximum contrast is $\kappa \approx 16$.

To fully resolve the microstructure on all 4096 ($n_H = 2^6$) coarse elements, we need to choose $n_h = 2^{13}$ which results in about 67.1 million degrees of freedom. The local corrector problems have a size of roughly 1.3 million degrees of freedom. With 1024 available parallel processes, each process must train ROMs for 4 coarse elements.

We choose a training set $\mathcal{P}_{\text{train}} \subset \mathcal{P}$ of 4^3 equidistant parameters and show results for $\varepsilon_1 = 0.01$ and $\varepsilon_2 = 0.02$ in Table 2. Again, the TSRBLOD shows high online efficiency with speed-ups of up to 10^6 , clearly outperforming the RBLOD. We note that the reported online time of $t^{\text{online}} = 4.39$ s for the RBLOD roughly splits into 2.2 s required for sequentially solving the reduced corrector problems (Step 1 in subsection 3.4), 1.2 s for assembling the coarse system (Step 2) and 1 s for solving the coarse system (Step 3). In particular, the further speed-up that could be achieved for the RBLOD by parallelizing the corrector problems is bounded by a factor of approximately 2.

Also, the storage requirements are noteworthy: the reduced data required for evaluating the

method	RBLOD	TSRBLOD
$t_1^{\text{offline}}(T)$	10278	11289
t_1^{offline}	49436	54837
t_2^{offline}	-	9206
t^{offline}	49436	64043
cum. size St.1	278528	193289
av. size St.1	17.00	47.19
size St.2	-	16
t^{LOD}	515	
t^{online}	4.39	0.0005
speed-up w.r.t LOD	117	9.57e5
$e_{\text{LOD}}^{H^1, \text{rel}}$	1.95e-5	4.43e-4
$e_{\text{LOD}}^{L^2, \text{rel}}$	2.36e-5	4.49e-4

Table 2: Performance, ROM sizes and accuracy of the methods for test case 2 with $\varepsilon_1 = 0.01$ and $\varepsilon_2 = 0.02$. All times are given in seconds.

TSRBLOD ROM and $\eta_{a,\mu}$ is only 28 KB in size, whereas the RBLOD requires 409 MB.

7 Concluding remarks and future work

In the work at hand, we have derived a new two-scale reduced scheme for the PG-LOD. Due to the two-stage reduction process and the independence of the resulting ROMs from the size of both the fine-scale and the coarse-scale meshes, our approach is effective even for large-scale problems. For ease of presentation, we have assumed non-parametric right-hand sides and did not consider output functionals. Incorporating both into our approach is straightforward. Furthermore, for very large coarse meshes, additional intermediate reduction stages could be added to further reduce the needed computational effort in Stage 2. Instead of a fixed a priori choice of the Stage 1 tolerance ε_1 , the Stage 1 ROMs could be adaptively enriched during Stage 2 when an insufficient approximation quality of some of the Stage 1 ROMs is detected. The presented methodology could also be applied to other problem classes and to other multiscale methods.

Code availability

All experiments have been implemented in Python using `gridlod` [18] for the PG-LOD discretization and `pyMOR` [30] for the Model Order Reduction. For the complete source code of all experiments including setup instructions, we refer to [26].

References

- [1] Assyr Abdulle and Yun Bai. Reduced basis finite element heterogeneous multiscale method for high-order discretizations of elliptic homogenization problems. *Journal of Computational Physics*, 231(21):7014–7036, 2012.
- [2] Assyr Abdulle and Yun Bai. Adaptive reduced basis finite element heterogeneous multiscale method. *Computer Methods in Applied Mechanics and Engineering*, 257:203–220, 2013.
- [3] Assyr Abdulle and Yun Bai. Reduced-order modelling numerical homogenization. *Philosophical Transactions of the Royal Society A: Mathematical, Physical and Engineering Sciences*, 372(2021):20130388, 2014.

- [4] Assyr Abdulle, Yun Bai, and Gilles Vilmart. An offline–online homogenization strategy to solve quasilinear two-scale problems at the cost of one-scale problems. *International Journal for Numerical Methods in Engineering*, 99(7):469–486, 2014.
- [5] Assyr Abdulle and Andrea Di Blasio. Numerical homogenization and model order reduction for multiscale inverse problems. *Multiscale Modeling & Simulation*, 17(1):399–433, 2019.
- [6] Assyr Abdulle and Patrick Henning. A reduced basis localized orthogonal decomposition. *Journal of Computational Physics*, 295:379–401, 2015.
- [7] Grégoire Allaire. Homogenization and two-scale convergence. *SIAM Journal on Mathematical Analysis*, 23(6):1482–1518, 1992.
- [8] Ivo Babuska and Robert Lipton. Optimal local approximation spaces for generalized finite element methods with application to multiscale problems. *Multiscale Modeling & Simulation*, 9(1):373–406, 2011.
- [9] Maxime Barrault, Yvon Maday, Ngoc C. Nguyen, and Anthony. T. Patera. An ‘empirical interpolation’ method: application to efficient reduced-basis discretization of partial differential equations. *C. R. Math. Acad. Sci. Paris*, 339(9):667–672, 2004.
- [10] Peter Binev, Albert Cohen, Wolfgang Dahmen, Ronald DeVore, Guergana Petrova, and Przemyslaw Wojtaszczyk. Convergence rates for greedy algorithms in reduced basis methods. *SIAM J. Math. Anal.*, 43(3):1457–1472, 2011.
- [11] Sébastien Boyaval. Reduced-basis approach for homogenization beyond the periodic setting. *Multiscale Modeling & Simulation*, 7(1):466–494, 2008.
- [12] Andreas Buhr, Christian Engwer, Mario Ohlberger, and Stephan Rave. A Numerically Stable A Posteriori Error Estimator for Reduced Basis Approximations of Elliptic Equations. In E. Oñate, X. Oliver, and A. Huerta, editors, *11th. World Congress on Computational Mechanics*, pages 4094–4102. International Center for Numerical Methods in Engineering, Barcelona, 2014.
- [13] Andreas Buhr, Laura Iapichino, Mario Ohlberger, Stephan Rave, Felix Schindler, and Kathrin Smetana. Localized model reduction for parameterized problems. In Peter Benner, Stefano Grivet-Talocia, Alfio Quarteroni, Gianluigi Rozza, Wilhelmus Schilders, and Luís Miguel Silveira, editors, *Model Order Reduction (Volume 2)*. De Gruyter, Berlin, Boston, 2021.
- [14] Yalchin Efendiev, Juan Galvis, and Thomas Y Hou. Generalized multiscale finite element methods (GMsFEM). *Journal of computational physics*, 251:116–135, 2013.
- [15] Yalchin Efendiev and Thomas Y Hou. *Multiscale finite element methods: theory and applications*, volume 4. Springer Science & Business Media, 2009.
- [16] Daniel Elfverson, Victor Ginting, and Patrick Henning. On multiscale methods in petrov–galerkin formulation. *Numerische Mathematik*, 131(4):643–682, 2015.
- [17] Bernard Haasdonk. Reduced basis methods for parametrized PDEs: A tutorial introduction for stationary and instationary problems. *Model reduction and approximation: theory and algorithms*, 15:65, 2017.
- [18] Fredrik Hellman and Tim Keil. gridlod. <https://github.com/fredrikhellman/gridlod>.
- [19] Fredrik Hellman, Tim Keil, and Axel Målqvist. Numerical upscaling of perturbed diffusion problems. *SIAM Journal on Scientific Computing*, 42(4):A2014–A2036, 2020.
- [20] Fredrik Hellman and Axel Målqvist. Contrast independent localization of multiscale problems. *Multiscale Modeling & Simulation*, 15(4):1325–1355, 2017.
- [21] Fredrik Hellman and Axel Målqvist. Numerical homogenization of elliptic pdes with similar coefficients. *Multiscale Modeling & Simulation*, 17(2):650–674, 2019.
- [22] Jan S Hesthaven, Gianluigi Rozza, and Benjamin Stamm. *Certified Reduced Basis Methods for Parametrized Partial Differential Equations*. SpringerBriefs in Mathematics. Springer International Publishing, Cham, 2016.
- [23] Jan S. Hesthaven, Shun Zhang, and Xueyu Zhu. Reduced Basis Multiscale Finite Element Methods for Elliptic Problems. *Multiscale Modeling & Simulation*, 13(1):316–337, 2015.
- [24] Thomas Y Hou and Xiao-Hui Wu. A multiscale finite element method for elliptic problems in composite materials and porous media. *Journal of computational physics*, 134(1):169–189, 1997.
- [25] T. J. R. Hughes, G. R. Feijóo, L. Mazzei, and J.-B. Quinicy. The variational multiscale method—a paradigm for computational mechanics. *Comput. Methods Appl. Mech. Engrg.*, 166(1-2):3–24, 1998.
- [26] Tim Keil and Stephan Rave. Software for "An Online Efficient Two-Scale Reduced Basis Approach for the Localized Orthogonal Decomposition". url: <https://doi.org/10.5281/zenodo.5705584>, November 2021.

- [27] Roland Maier and Barbara Verfürth. Multiscale scattering in nonlinear kerr-type media. *arXiv preprint arXiv:2011.09168*, 2020.
- [28] Axel Målqvist and Daniel Peterseim. Localization of elliptic multiscale problems. *Mathematics of Computation*, 83(290):2583–2603, 2014.
- [29] Axel Målqvist and Daniel Peterseim. *Numerical Homogenization by Localized Orthogonal Decomposition*. SIAM, 2020.
- [30] René Milk, Stephan Rave, and Felix Schindler. pyMOR – Generic Algorithms and Interfaces for Model Order Reduction. *SIAM Journal on Scientific Computing*, 38(5):S194–S216, 2016.
- [31] Axel Målqvist and Barbara Verfürth. An offline-online strategy for multiscale problems with random defects, 2021.
- [32] Ngoc C. Nguyen. A multiscale reduced-basis method for parametrized elliptic partial differential equations with multiple scales. *Journal of Computational Physics*, 227(23):9807–9822, 2008.
- [33] Mario Ohlberger. A posteriori error estimates for the heterogeneous multiscale finite element method for elliptic homogenization problems. *Multiscale Modeling & Simulation*, 4(1):88–114, 2005.
- [34] Mario Ohlberger and Michael Schaefer. A reduced basis method for parameter optimization of multiscale problems. In *Proceedings of ALGORITMY*, volume 2012, pages 1–10, 2012.
- [35] Mario Ohlberger and Michael Schaefer. Error control based model reduction for parameter optimization of elliptic homogenization problems. *IFAC Proceedings Volumes*, 46(26):251–256, 2013.
- [36] Mario Ohlberger, Michael Schaefer, and Felix Schindler. Localized Model Reduction in PDE Constrained Optimization. In Volker Schulz and Diaraf Seck, editors, *Shape Optimization, Homogenization and Optimal Control : DFG-AIMS Workshop Held at the AIMS Center Senegal, March 13-16, 2017*, International Series of Numerical Mathematics, pages 143–163. Springer International Publishing, Cham, 2018.
- [37] Daniel Peterseim. Variational multiscale stabilization and the exponential decay of fine-scale correctors. In *Building bridges: connections and challenges in modern approaches to numerical partial differential equations*, pages 343–369. Springer, 2016.
- [38] Daniel Peterseim and Robert Scheichl. Robust numerical upscaling of elliptic multiscale problems at high contrast. *Computational Methods in Applied Mathematics*, 16(4):579–603, 2016.
- [39] Alfio Quarteroni, Andrea Manzoni, and Federico Negri. *Reduced Basis Methods for Partial Differential Equations*, volume 92 of *UNITEXT*. Springer International Publishing, Cham, 2016.
- [40] E Weinan, Björn Engquist, and Zhongyi Huang. Heterogeneous multiscale method: a general methodology for multiscale modeling. *Physical Review B*, 67(9):092101, 2003.